LETTER

doi:10.1038/nature20789

Splicing factor 1 modulates dietary restriction and TORC1 pathway longevity in *C. elegans*

Caroline Heintz[1], Thomas K. Doktor[2]*, Anne Lanjuin[1]*, Caroline C. Escoubas[1,3], Yue Zhang[1], Heather J. Weir[1], Sneha Dutta[1], Carlos Giovanni Silva-García[1], Gitte H. Bruun[2], Ianessa Morantte[1]†, Gerta Hoxhaj[1], Brendan D. Manning[1], Brage S. Andresen[2] & William B. Mair[1]

Ageing is driven by a loss of transcriptional and protein homeostasis[1–3] and is the key risk factor for multiple chronic diseases. Interventions that attenuate or reverse systemic dysfunction associated with age therefore have the potential to reduce overall disease risk in the elderly. Precursor mRNA (pre-mRNA) splicing is a fundamental link between gene expression and the proteome, and deregulation of the splicing machinery is linked to several age-related chronic illnesses[4,5]. However, the role of splicing homeostasis in healthy ageing remains unclear. Here we demonstrate that pre-mRNA splicing homeostasis is a biomarker and predictor of life expectancy in *Caenorhabditis elegans*. Using transcriptomics and in-depth splicing analysis in young and old animals fed *ad libitum* or subjected to dietary restriction, we find defects in global pre-mRNA splicing with age that are reduced by dietary restriction via splicing factor 1 (SFA-1; the *C. elegans* homologue of SF1, also known as branchpoint binding protein, BBP). We show that SFA-1 is specifically required for lifespan extension by dietary restriction and by modulation of the TORC1 pathway components AMPK, RAGA-1 and RSKS-1/S6 kinase. We also demonstrate that overexpression of SFA-1 is sufficient to extend lifespan. Together, these data demonstrate a role for RNA splicing homeostasis in dietary restriction longevity and suggest that modulation of specific spliceosome components may prolong healthy ageing.

Expression of specific RNA splicing factors has recently been shown to correlate with longevity in *C. elegans*, mice and humans[6–11], yet links between RNA splicing and the promotion of healthy ageing via interventions such as dietary restriction are unclear. To examine the role of pre-mRNA splicing in dietary restriction using a multicellular system, we used an *in vivo* fluorescent alternative splicing reporter in the nematode *C. elegans*. This reporter strain expresses a pair of *ret-1* exon 5 reporter minigenes with differential frameshifts, driven by the ubiquitous *eft-3* promoter[12]. GFP expression indicates that exon 5 has been included, whereas expression of mCherry indicates that exon 5 has been skipped (Fig. 1a) and live imaging reveals cell- and tissue-specific *ret-1* alternative splicing[12] (Fig. 1b, Extended Data Fig. 1a). We examined whether the reporter responded to spliceosome disruption by inhibiting multiple, conserved[13] spliceosome components by RNA interference (RNAi) (Extended Data Fig. 1b–o). RNAi of *hrp-2*, a core spliceosome component in *C. elegans* and mammals, completely deregulates *ret-1* exon inclusion on the first day of the adult stage (day 1) (Extended Data Fig. 1d, e). RNA sequencing of *hrp-2*-RNAi-treated animals showed altered splicing of the endogenous *ret-1* gene (Extended Data Fig. 2a, b), as well as widespread splicing defects, including intron retention, exon skipping, and differentially regulated alternative splicing (Extended Data Fig. 2c–f, Supplementary Table 1). Deregulation of the splicing reporter therefore correlates with loss of endogenous splicing fidelity *in vivo* in *C. elegans*.

We next used the splicing reporter to monitor alternative splicing in ageing animals. Splicing in *C. elegans* is under tight regulation, especially during development[13,14]. As a result, the splicing reporter undergoes stereotypical tissue-specific changes in alternative splicing throughout larval development that are homogeneous across the population[12]. However, by day 5, when *C. elegans* are still considered 'youthful'[15] and are phenotypically homogeneous under bright-field microscopy, we observed heterogeneous patterns of exon usage both between individuals and between the same cell types within individuals (Fig. 1c, d). This is especially evident within cells of the intestine, which stochastically begin to skip exon 5 and therefore express mCherry. By day 7, all animals lose youthful splicing patterns, with cells of the intestine showing differential exon skipping (Fig. 1d), despite the reporter minigene being robustly expressed in old animals (Extended Data Fig. 2g). Ageing therefore leads to a deregulation in alternative splicing and this occurs at different rates between individuals.

We analysed the effects of dietary restriction on *ret-1* splicing using a solid-plate dietary restriction (sDR) regime that robustly extends lifespan[16] (65% lifespan increase, $P < 0.0001$, Extended Data Fig. 2h). While animals fed *ad libitum* show deregulated *ret-1* splicing with age, *C. elegans* on sDR maintain a youthful splicing pattern and maintain population homogeneity (Fig. 1e, Extended Data Fig. 2i). Despite being isogenic, wild-type *C. elegans* fed *ad libitum* show remarkable heterogeneity in rates of ageing between individuals. To determine whether inter-individual splicing variation might underlie inter-individual differences in wild-type ageing, we sorted age-synchronized (day 6) *C. elegans* fed *ad libitum* into two groups, based solely on their splicing patterns: A, animals with increased exon 5 skipping reminiscent of old worms fed *ad libitum*; and B, animals with increased exon 5 inclusion characteristic of *C. elegans* on a restricted diet (Fig. 1f, Extended Data Fig. 2j). Notably, the subsequent median lifespan of *C. elegans* in group B was significantly greater than those in group A that exhibited early-onset deregulated alternative splicing (23% increased, $P < 0.0001$, Fig. 1g). Therefore, splicing efficiency declines more rapidly in *C. elegans* fed *ad libitum* than in those on dietary restriction, and specific splicing events can be used as a predictor of subsequent life expectancy in young animals.

To determine whether splicing fidelity contributes to the effect of dietary restriction on ageing, we performed a targeted reverse genetic screen for spliceosome components that affect lifespan during wild-type or restricted feeding using the *eat-2(ad1116)* mutant as a genetic model for dietary restriction[17]. We selected conserved splicing factors representing both core components of the spliceosome, as well as RNA-binding proteins including SR and hnRNP protein family members

[1]Department of Genetics and Complex Diseases, Harvard T. H. Chan School of Public Health, Boston, Massachusetts 02115, USA. [2]Department of Biochemistry and Molecular Biology, and Villum Center for Bioanalytical Sciences, University of Southern Denmark, 5230 Odense, Denmark. [3]Institute for Research on Cancer and Aging, Nice (IRCAN), CNRS, UMR7284, INSERM U1081, University of Nice Sophia Antipolis, Faculty of Medicine, 06107 Nice, France. †Present address: Laboratory of Neurophysiology and Behavior, The Rockefeller University, New York City, New York 10065, USA.
*These authors contributed equally to this work.

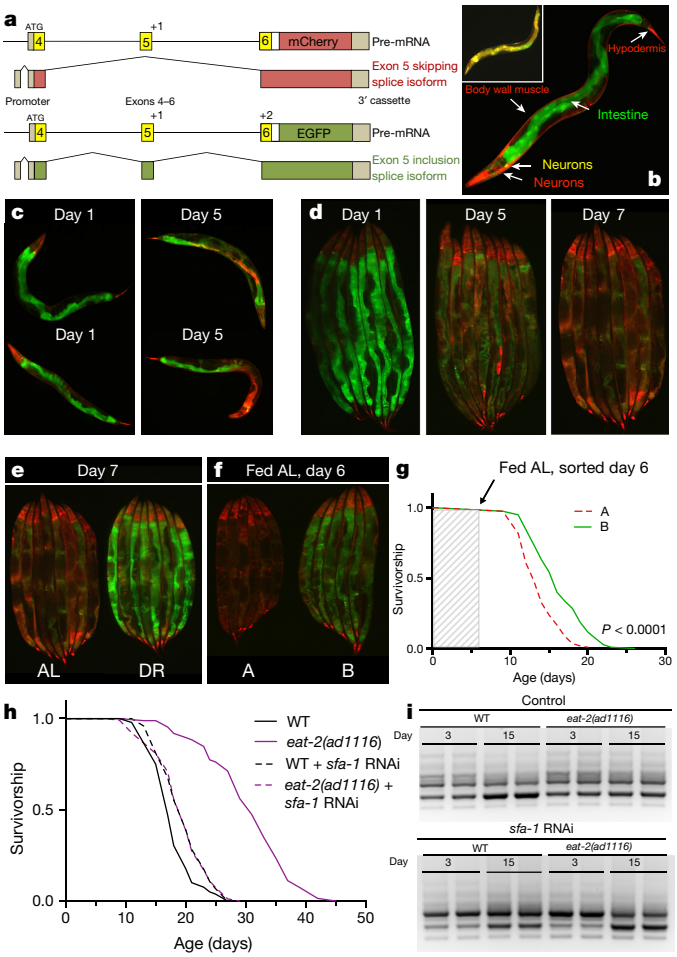

Figure 1 | The role of RNA splicing in dietary restriction longevity. **a**, Schematic of the *ret-1* splicing reporter[12]. **b**, Tissue-specific *ret-1* splicing in day 1 *C. elegans*. Inset, control reporter without frameshifts. 10× magnification. **c**, **d**, Representative reporter splicing at days 1 and 5 (**c**), and days 1, 5 and 7 (**d**). **e**, Splicing reporter worms fed *ad libitum* (AL) or on dietary restriction (DR) at day 7. **f**, Representative images of age-matched animals in group A (increased exon 5 skipping) and group B (increased exon 5 inclusion). **g**, Survivorship of groups A and B. Arrow denotes sorting day ($P < 0.0001$, 1 of 2 replicates). **h**, Survivorship of wild-type (WT) and *eat-2(ad1116)* animals with or without *sfa-1* RNAi ($P = 0.9783$, *ad libitum* feeding with *sfa-1* RNAi versus dietary restriction with *sfa-1* RNAi, 7 replicates). **i**, *tos-1* isoforms in wild-type and *eat-2(ad1116)* worms with or without *sfa-1* RNAi (day 3 versus 15, $n = 2$ biological replicates). Lifespans, $n = 100$ worms per condition; *P* values calculated with log-rank test.

(Extended Data Fig. 1c)[13]. We identified spliceosome components whose inhibition significantly reduced lifespan of both wild-type and dietary-restricted animals and factors that did not affect longevity (Extended Data Fig. 2k–p, Extended Data Table 1). Notably, however, RNAi of the branch-point binding protein splicing factor 1 (SFA-1)[18] completely abolishes any extension of lifespan by dietary restriction (*ad libitum* feeding with *sfa-1* RNAi versus dietary restriction with *sfa-1* RNAi: $P = 0.9783$, log-rank, Fig. 1h) yet did not shorten wild-type lifespan. *sfa-1* RNAi reduced *sfa-1* expression by 50% but did not affect expression of *uaf-2*, which is co-transcribed in an operon with *sfa-1* (Extended Data Fig. 3a). *sfa-1* RNAi also has no effect on feeding/pumping rates in *C. elegans* (Extended Data Fig. 3b, c). We analysed the splicing pattern of a known target of SFA-1, target of splicing (*tos-1*)[19,20], to assay changes in SFA-1 activity with age and dietary restriction. PCR analysis revealed an age-associated change in *tos-1* isoform splicing that is prevented by dietary restriction in an SFA-1-dependent manner (Fig. 1i). In addition, *sfa-1* RNAi blocked the effect of dietary restriction on age-related changes to *ret-1* splicing as assayed both by the *in vivo* reporter and by PCR of endogenous *ret-1* (Extended Data Fig. 3d, e). Together, these data demonstrate a role for SFA-1 and RNA processing in lifespan extension by dietary restriction.

Next, we performed unbiased analyses of the effect of age, dietary restriction and SFA-1 on global RNA processing and gene expression, to investigate the mechanism by which SFA-1 promotes dietary restriction longevity. We performed 100 bp paired-end RNA-seq on samples taken from young and old worms fed *ad libitum* (N2 strain) or on dietary restriction (*eat-2(ad1116)*, DA1116 strain) with or without RNAi for *sfa-1*, in parallel to assaying their lifespan. Samples were collected at day 3 when no animals had died, at day 15 (*ad libitum* and dietary restriction *sfa-1* RNAi, 75% survival; dietary restriction alone, 100% survival), and day 27 (dietary restriction, 75% survival) (Fig. 2a). This design allowed us to match groups with the same chronological age (coloured vertical lines) and physiological age (horizontal dashed line). Gene expression changes and splicing events identified by the RNA-seq, including age-related changes to endogenous *ret-1* and *tos-1*, were validated with semi-quantitative and quantitative reverse transcription PCR (qRT–PCR) (Extended Data Figs 4, 5, Supplementary Tables 2–5).

We assessed the effect of age on multiple parameters of pre-mRNA processing in *C. elegans* fed *ad libitum* and on dietary restriction. We did not detect universal changes in splicing factor expression with age (Supplementary Table 6). However, ageing induced hallmarks of global spliceosome disruption; day 15 animals fed *ad libitum* showed a significant increase in both intron retention and unannotated splice junctions indicative of increased splicing noise with age (Fig. 2b). Dietary restriction reduced the increase in alternative splicing events detected with age (Extended Data Fig. 6a), while multidimensional scaling analysis of all differential splicing events over age suggests that dietary restriction reduces splicing heterogeneity (Extended Data Fig. 6b). Dietary-restricted animals also expressed fewer novel splicing events compared to *ad libitum* controls (Extended Data Fig. 6c, Supplementary Table 7). Moreover, dietary restriction protected against age-induced deregulation of pre-mRNA processing; day 15 animals on dietary restriction did not show significant increases in either intron retention or unannotated splice junctions compared to day 3 (Fig. 2c). By day 27, however, when the physiological age of dietary-restricted animals matched that of day 15 worms fed *ad libitum*, both parameters of spliceosome dysfunction were significantly increased (Fig. 2c). Suggesting a role for SFA-1 in the effect of dietary restriction on global RNA processing, dietary restriction no longer suppressed age-related increases in unannotated splice junctions or total alternative splicing events in animals with *sfa-1* RNAi (Fig. 2d, Extended Data Fig. 6d). Together, these data suggest that dietary restriction protects against dysfunctional processing of specific pre-mRNAs seen with age, and that this protection requires SFA-1.

To define the effects of dietary restriction that are specifically modulated by SFA-1, we first analysed differential gene expression changes between animals fed *ad libitum* and animals on dietary restriction at day 15, with and without *sfa-1* RNAi (Supplementary Tables 4, 5). We then determined the KEGG pathways significantly altered by dietary restriction in day 15 animals in an SFA-1-dependent manner. RNAi of *sfa-1* did not block all dietary restriction-related changes to gene expression, but instead specifically reversed upregulation of lipid/fatty acid metabolism genes induced by dietary restriction (Fig. 3a, boxed region, Extended Data Fig. 6e, f). Further, Gene Ontology analysis of genes showing intron inclusion with age in both *ad libitum* and dietary restriction plus *sfa-1* RNAi conditions, but not in dietary restriction alone, are functionally enriched for metabolic processes including lipid catabolism and carbohydrate transport (Fig. 3b, Supplementary Table 8). We next asked whether SFA-1 modulates the effects of dietary restriction on metabolism directly, by measuring oxygen consumption in live young (day 4) and old (day 15) *C. elegans* fed *ad libitum* or on dietary restriction with and without *sfa-1* RNAi (Fig. 3c). Animals fed *ad libitum* showed decreased maximal

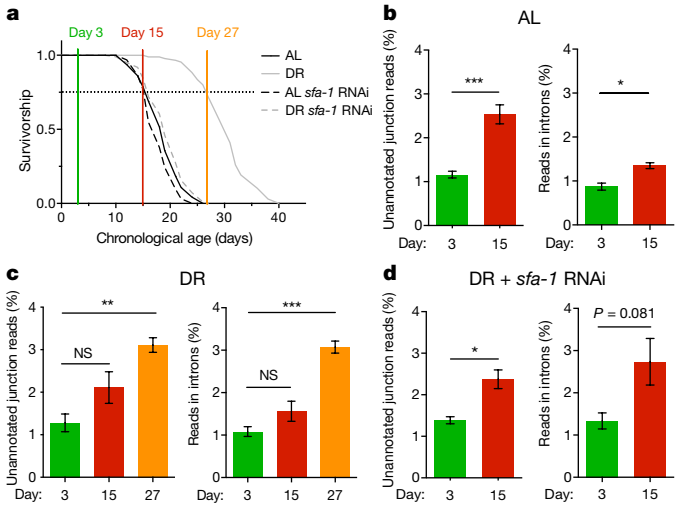

Figure 2 | Dietary restriction promotes genome-wide splicing efficiency. a, Survivorship of worms fed *ad libitum* or on dietary restriction (*eat-2(ad1116)*) with or without *sfa-1* RNAi collected for RNA-seq. Vertical lines signify chronological ages of sample collections. Horizontal dashed line signifies a physiological age; the survival curves for *ad libitum*, dietary restricted *sfa-1* RNAi and *ad libitum sfa-1* RNAi worms reach this physiological age earlier (Day 15) than dietary restricted worms (Day 27). **b**, By day 15, feeding *ad libitum* significantly increases unannotated junction reads (***$P = 0.0006$) and intron retention (*$P = 0.0106$) compared to day 3. **c**, There is no such significant increase in unannotated junction reads or intron retention between day 3 and 15 in dietary restricted animals ($P > 0.05$ in each case). By day 27, dietary restricted worms have significantly increased unannotated junction reads (**$P = 0.0036$) and intron retention (***$P = 0.0004$) compared to day 3. **d**, Unannotated junction reads and intron reads in dietary restricted animals with *sfa-1* RNAi (day 15 versus 3, **$P = 0.0065$, NS, $P > 0.05$). Mean ± s.e.m., per cent of total reads shown (**b**–**d**). *P* values in panels **b**–**d** calculated with unpaired, two-tailed *t*-test after probit transformation. Four biological replicate populations collected for RNA-seq. Lifespans, $n = 100$ worms per condition.

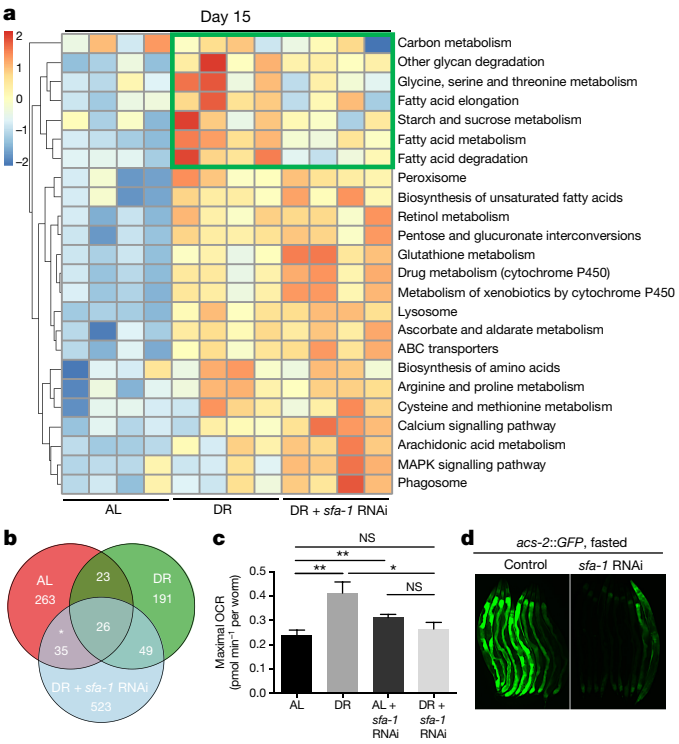

Figure 3 | SFA-1 regulates metabolic effects of dietary restriction. **a**, Heat map of KEGG pathway analysis in wild-type worms fed *ad libitum*, animals on dietary restriction and dietary restriction with *sfa-1* RNAi at day 15. **b**, Venn diagram representing intron inclusion events at day 15 in worms fed *ad libitum*, animals on dietary restriction and dietary restriction with *sfa-1* RNAi (*GO analysis in Supplementary Table 8). **c**, Maximal respiratory capacity (day 15 normalized to day 4, mean + s.e.m., **$P < 0.01$, *$P < 0.05$, NS, not significant, unpaired, two-tailed *t*-test, $n = 100$ animals per condition). **d**, Transcriptional induction of *acs-2P::GFP* in control and *sfa-1* knockdown worms after 23 h of fasting (representative image of two experiments shown).

respiratory capacity with age, and this decline is attenuated by dietary restriction in an SFA-1-dependent manner (Fig. 3c, Extended Data Fig. 6g, h). In addition, *sfa-1* RNAi blocked fasting-induced expression of acyl-CoA synthetase, which is critical for fatty acid oxidation during starvation (Fig. 3d and Extended Data Fig. 6i, j). To determine whether the effect of SFA-1 on metabolic gene expression was unique to *C. elegans*, we performed RNA-seq in HeLa cells with and without short interfering RNA (siRNA) of the mammalian SFA-1 orthologue, splicing factor 1 (SF1). Supporting a conserved role for SF1 in metabolic regulation from worms to mammals, in addition to defects in splicing, the most statistically significantly enriched KEGG pathways in HeLa cells with SF1 siRNA are metabolic processes (Extended Data Fig. 7, Supplementary Table 9). Together these data suggest a role for SFA-1 in metabolic plasticity and mitochondrial function during dietary restriction.

In order to identify putative mechanisms linking dietary restriction to splicing, we crossed the *ret-1* minigene reporter into animals carrying null mutations in genes linked to dietary-restriction-mediated longevity[21]: *aak-2*, a catalytic subunit of the energy sensor AMP-activated protein kinase (AMPK); *daf-16*, a forkhead transcription factor; or *raga-1*, a Rag GTPase that links amino acid sensing to mechanistic target of rapamycin complex 1 (mTORC1) activity. Dietary restriction maintained homogenous *ret-1* splicing patterns in old (day 8) *C. elegans* lacking AAK-2 or DAF-16, similar to that seen in dietary-restricted wild-type worms (Fig. 4a, b, Extended Data Fig. 8a, b). Notably, the *raga-1(ok386)* mutation completely abolishes the effects of dietary restriction on *ret-1* splicing with age (Fig. 4c, Extended Data Fig. 8c), without affecting *ret-1* splicing in early adulthood (Extended Data Fig. 8d). In addition, *raga-1(ok386)* mutants show decreased phosphorylation of the mTORC1 target RSKS-1/S6 kinase, and block the effects of age on SFA-1 activity as assayed by *tos-1* splicing (Extended Data Fig. 8e, f). These data therefore suggest that amino acid sensing by RAGA-1 is a critical link between dietary restriction and the regulation of pre-mRNA splicing homeostasis.

Direct suppression of mTORC1 increases lifespan, and mTORC1 is implicated as a mediator of the beneficial effects of dietary restriction. We therefore tested the role of SFA-1 in lifespan extension via suppression of multiple mTORC1 pathway components. Notably, *sfa-1* RNAi fully suppresses lifespan extension via null mutations in both *raga-1* (Fig. 4d) and *rsks-1* (Fig. 4e). mTORC1 integrates insulin/insulin-like growth factor 1 (IIS) signalling and AMPK-mediated energy sensing[22]. *sfa-1* RNAi fully suppresses lifespan extension via constitutive AAK-2 activation (Extended Data Fig. 8g), but does not fully suppress increased longevity of *daf-2(e1370)* mutants that have reduced IIS (Extended Data Fig. 8h). These data suggest that the role of SFA-1 extends beyond RAGA-1 as a general regulator of TORC1 pathway components, including AMPK, RAGA-1 and RSKS-1/S6 kinase.

The mechanisms linking TORC1 longevity and SFA-1 are unknown. Dynamic phosphorylation of splicing factors is essential to splicing regulation and spliceosomal activity[23] and deregulation of TORC pathway components with age may therefore result in aberrant splicing. However, although an mTOR consensus motif was identified in the mammalian orthologue of SFA-1, SF1(refs 24, 25), inhibition of TORC1 via rapamycin or torin has no effect on total SF1 levels in mouse

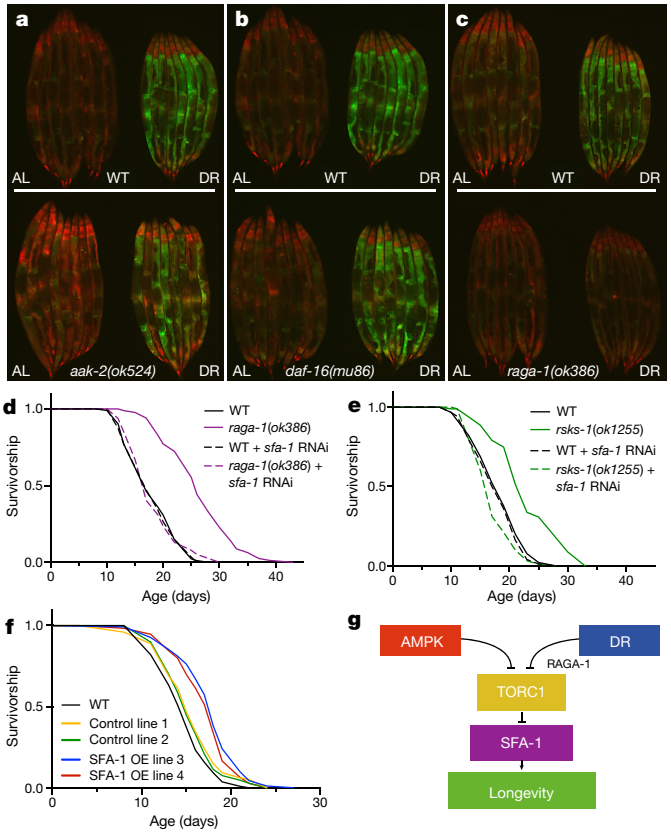

Figure 4 | SFA-1 promotes longevity. a–c, Splicing reporter in worms fed *ad libitum* (left) or on dietary restriction (right) at day 8 in *aak-2(ok524)* (**a**), *daf-16(mu86)* (**b**) or *raga-1(ok386)* (**c**) mutant backgrounds. Images are representative of at least two independent experiments. **d**, Effect of *sfa-1* RNAi on *raga-1(ok386)* mutant lifespan ($P = 0.6733$ versus wild type with *sfa-1* RNAi, 9 replicates). **e**, Lifespan analysis of *sfa-1* RNAi in long-lived *rsks-1(ok1255)* ($P = 0.0944$ versus wild type with *sfa-1* RNAi, 3 replicates). **f**, Overexpression (OE) of SFA-1 increases wild-type lifespan ($P < 0.0001$, 4 replicates). **g**, Model for the role of SFA-1 in dietary restriction and mTORC1 pathway longevity. *P* values calculated with log-rank test, $n = 100$ worms per condition.

embryonic fibroblasts, nor did we see SF1 gel shifts indicative of altered phosphorylation, as observed for the canonical TORC1 target S6 kinase (Extended Data Fig. 8i, j). Full characterization of spliceosome composition along with splicing factor protein levels, post-translational modifications with age and mTORC1 modulation represent important future directions for research.

SF1/BBP is required for early spliceosome assembly[26], yet it is not required for splicing of all pre-mRNAs[27] and has also been reported to function as a transcriptional suppressor[28]. How SFA-1 modulates dietary restriction and mTORC1 pathway longevity remains unclear. Several lines of evidence support a specific functional role for SFA-1 in promoting dietary restriction and mTORC1 longevity. First, inhibition of the nonsense-mediated decay pathway, a key RNA homeostatic mechanism, does not block lifespan extension by *raga-1* RNAi (Extended Data Fig. 9a) in *C. elegans*. Second, we identified an additional splicing factor, REPO-1, that is required for dietary restriction longevity but unlike SFA-1 is completely dispensable for *raga-1* lifespan (Extended Data Fig. 9b-d). Notably however, both SFA-1 and REPO-1 are required for lifespan extension via modulation of mitochondrial electron transport chain components (Extended Data Fig. 9e, f), raising the prospect that differential composition of the spliceosome and specific splicing factors might mediate alternative longevity pathways. Finally, moderate overexpression of *sfa-1* in *C. elegans* modifies *tos-1* splicing and is sufficient to increase lifespan by 15–33% (Fig. 4f, $P < 0.0001$, Extended Data Fig. 9g–i). Together, these data suggest that SFA-1 might be targeted to promote healthy ageing and highlight an emerging role for pre-mRNA splicing in lifespan extension via mTORC1 suppression and dietary restriction (Fig. 4g). Further, interventions that suppress mTORC1 and mimic dietary restriction might provide new therapeutic avenues for human RNA-splicing-related diseases.

Online Content Methods, along with any additional Extended Data display items and Source Data, are available in the online version of the paper; references unique to these sections appear only in the online paper.

Received 30 September 2015; accepted 15 November 2016.
Published online 5 December 2016.

1. Kenyon, C. J. The genetics of ageing. *Nature* **464,** 504–512 (2010).
2. Taylor, R. C. & Dillin, A. Aging as an event of proteostasis collapse. *Cold Spring Harb. Perspect. Biol.* **3,** a004440 (2011).
3. Vermulst, M. *et al.* Transcription errors induce proteotoxic stress and shorten cellular lifespan. *Nat. Commun.* **6,** 8065 (2015).
4. Wang, G.-S. & Cooper, T. A. Splicing in disease: disruption of the splicing code and the decoding machinery. *Nat. Rev. Genet.* **8,** 749–761 (2007).
5. Singh, R. K. & Cooper, T. A. Pre-mRNA splicing in disease and therapeutics. *Trends Mol. Med.* **18,** 472–482 (2012).
6. Lee, B. P. *et al.* Changes in the expression of splicing factor transcripts and variations in alternative splicing are associated with lifespan in mice and humans. *Aging Cell* **15,** 903–913 (2016).
7. Seo, M., Park, S., Nam, H. & Lee, S.-J. RNA helicase SACY-1 is required for longevity caused by various genetic perturbations in *Caenorhabditis elegans*. *Cell Cycle* **15,** 1821–1829 (2016).
8. Rodríguez, S. A. *et al.* Global genome splicing analysis reveals an increased number of alternatively spliced genes with aging. *Aging Cell* **15,** 267–278 (2016).
9. Curran, S. P. & Ruvkun, G. Lifespan regulation by evolutionarily conserved genes essential for viability. *PLoS Genet.* **3,** e56 (2007).
10. Gao, X. *et al.* The survival motor neuron gene smn-1 interacts with the U2AF large subunit gene uaf-1 to regulate *Caenorhabditis elegans* lifespan and motor functions. *RNA Biol.* **11,** 1148–1160 (2014).
11. Zhang, T., Hwang, H.-Y., Hao, H., Talbot, C., Jr & Wang, J. *Caenorhabditis elegans* RNA-processing protein TDP-1 regulates protein homeostasis and life span. *J. Biol. Chem.* **287,** 8371–8382 (2012).
12. Kuroyanagi, H., Watanabe, Y., Suzuki, Y. & Hagiwara, M. Position-dependent and neuron-specific splicing regulation by the CELF family RNA-binding protein UNC-75 in *Caenorhabditis elegans*. *Nucleic Acids Res.* **41,** 4015–4025 (2013).
13. Zahler, A. Pre-mRNA splicing and its regulation in *Caenorhabditis elegans*. *Wormbook* http://dx.doi.org/10.1895/wormbook.1.31.2 (2012).
14. Ramani, A. K. *et al.* Genome-wide analysis of alternative splicing in *Caenorhabditis elegans*. *Genome Res.* **21,** 342–348 (2011).
15. Herndon, L. A. *et al.* Stochastic and genetic factors influence tissue-specific decline in ageing *C. elegans*. *Nature* **419,** 808–814 (2002).
16. Ching, T.-T. T. & Hsu, A.-L. L. Solid plate-based dietary restriction in *Caenorhabditis elegans*. *J. Vis. Exp.* (51):2701 (2011).
17. Lakowski, B. & Hekimi, S. The genetics of caloric restriction in *Caenorhabditis elegans*. *Proc. Natl Acad. Sci. USA* **95,** 13091–13096 (1998).
18. Krämer, A. Purification of splicing factor SF1, a heat-stable protein that functions in the assembly of a presplicing complex. *Mol. Cell. Biol.* **12,** 4545–4552 (1992).
19. Ma, L. & Horvitz, H. R. Mutations in the *Caenorhabditis elegans* U2AF large subunit UAF-1 alter the choice of a 3′ splice site *in vivo*. *PLoS Genet.* **5,** e1000708 (2009).
20. Ma, L., Tan, Z., Teng, Y., Hoersch, S. & Horvitz, H. R. *In vivo* effects on intron retention and exon skipping by the U2AF large subunit and SF1/BBP in the nematode *Caenorhabditis elegans*. *RNA* **17,** 2201–2211 (2011).
21. Fontana, L., Partridge, L. & Longo, V. D. Extending healthy life span--from yeast to humans. *Science* **328,** 321–326 (2010).
22. Johnson, S. C., Rabinovitch, P. S. & Kaeberlein, M. mTOR is a key modulator of ageing and age-related disease. *Nature* **493,** 338–345 (2013).
23. Stamm, S. Regulation of alternative splicing by reversible protein phosphorylation. *J. Biol. Chem.* **283,** 1223–1227 (2008).
24. Yu, Y. *et al.* Phosphoproteomic analysis identifies Grb10 as an mTORC1 substrate that negatively regulates insulin signaling. *Science* **332,** 1322–1326 (2011).
25. Hsu, P. P. *et al.* The mTOR-regulated phosphoproteome reveals a mechanism of mTORC1-mediated inhibition of growth factor signaling. *Science* **332,** 1317–1322 (2011).
26. Wang, X. *et al.* Phosphorylation of splicing factor SF1 on Ser20 by cGMP-dependent protein kinase regulates spliceosome assembly. *EMBO J.* **18,** 4549–4559 (1999).
27. Tanackovic, G. & Krämer, A. Human splicing factor SF3a, but not SF1, is essential for pre-mRNA splicing *in vivo*. *Mol. Biol. Cell* **16,** 1366–1377 (2005).
28. Zhang, D., Paley, A. J. & Childs, G. The transcriptional repressor ZFM1 interacts with and modulates the ability of EWS to activate transcription. *J. Biol. Chem.* **273,** 18086–18091 (1998).

Supplementary Information is available in the online version of the paper.

Acknowledgements C.H. is supported by the Swiss National Science Foundation (P2ZHP3_151609) and the Fonds National de la Recherche Luxembourg (AFR7883116). W.B.M. is funded by The Lawrence Ellison Medical Foundation (U54CA155626), The Glenn Foundation for Medical Research and the National Institutes of Health (NIH, 1R01AG044346). C.E. is supported by the Ligue Nationale contre le Cancer. G.H.B and T.K.D. were supported through a grant to B.S.A. from The Novo Nordisk Foundation (NNF13OC0007939). We are grateful to H. Kuroyanagi for providing the splicing reporter strain and corresponding plasmids. We thank K. Blackwell for providing the *glp-4* mutant strain and RNAi constructs. We also thank the *Caenorhabditis* Genetics Center for providing worm strains. We also thank the Mair laboratory members for comments and discussion on the project and manuscript.

Author Contributions C.H. and W.B.M. designed the study, C.H. performed the majority of the experiments and analysed results, A.L. performed experiments and edited the manuscript. T.K.D. analysed all the RNA-seq data. C.C.E., C.G.S.-G. and S.D. performed lifespan repeats and *C. elegans* sample collections, I.M. helped with cloning and crosses. H.J.W. performed the oxygen consumption experiments. G.H.B. and B.S.A. designed and performed the HeLa cells experiments including the sequencing run. Y.Z., G.H. and B.D.M. designed and performed the MEF and *C. elegans* immunoblotting experiments. C.H. and W.B.M. wrote the manuscript implementing comments and edits from all authors.

Author Information Reprints and permissions information is available at www.nature.com/reprints. The authors declare no competing financial interests. Readers are welcome to comment on the online version of the paper. Correspondence and requests for materials should be addressed to W.B.M. (wmair@hsph.harvard.edu).

Reviewer Information *Nature* thanks M. Kaeberlein, N. Tavernarakis and the other anonymous reviewer(s) for their contribution to the peer review of this work.

METHODS

No statistical methods were used to predetermine sample size. Investigators were blinded for worm strains and RNAi treatments where applicable for lifespan analyses in Figs. 1g, 4f and multiple lifespan repeats.

Worm strains and culture. The following *C. elegans* strains were obtained from the *Caenorhabditis* Genetic Center, funded by the NIH Office of Research Infrastructure Programs (P40 OD010440): N2 Bristol wild-type, DA1116 (*eat-2(ad1116)II*), RB754 (*aak-2(ok524)X*), MQ887 (*isp-1(qm150)IV*), VC222 (*raga-1(ok386)II*), and RB1206 (*rsks-1(ok1255)III*); three latter strains made by groups part of the International *C. elegans* Knockout Consortium. The generation of CA AMPK and *acs-2p::GFP* transcriptional reporter strains has been described previously[29,30]. CF1038 (*daf-16(mu86)I*) and CF1041 (*daf-2(e1370)III*) were obtained from the Kenyon laboratory via the Dillin laboratory. The SS104 (*glp-4(bn2)*) strain was a gift from K. Blackwell. The splicing reporter strain KH2235 (lin-15(n765)ybIs2167[eft-3p::ret-1E4E5(+1)E6-GGS6-mCherry+ eft-3p::ret-1E4E5(+1)E6(+2)GGS6-GFP+lin-15(+)+pRG5271Neo]X) was a gift from H. Kuroyanagi. Artificial frameshifts were introduced to prevent mCherry or EGFP expression when exon 5 is included (mCherry) or skipped (EGFP), respectively. The nervous system, body wall muscles, and hypodermis predominantly express ΔE5-mCherry, while pharynx and intestine predominantly express E5-EGFP. The inverted splicing reporter WBM535 was made by injecting modified minigene reporter plasmids into N2 worms. The inverted fluorophore plasmids were made by deleting the (+2) frameshift in the EGFP minigene and inserting a (+2) frameshift into the mCherry minigene. Control strain without minigene expresses two plasmids with *eft-3p::gfp* and *eft-3p::mCherry* ubiquitously.

Worms were routinely grown and maintained on standard nematode growth media (NGM) seeded with *E. coli* (OP50-1). *E. coli* bacteria were cultured overnight in LB at 37 °C, after which 100 µl of liquid culture was seeded on plates to grow for two days at room temperature. Use of 5-fluoro-2′-deoxyuridine (FUDR, 100 µl of 1 mg ml^{-1} solution, spotted on top of the bacterial lawn, 24 h before using the plates) to prevent excessive censoring, is noted in the legends of respective experiments.

Lifespans. All lifespan experiments were conducted at 20 °C unless otherwise noted in figure legend. Lifespan experiments were performed as described in Burkewitz *et al.*[30]. Graphpad Prism 6 was used to plot survival curves and determine median lifespan. Lifespan experiments began with $n = 100$ worms in each group. Survival curves were compared and *P* values calculated using the log-rank (Mantel–Cox) analysis method. Complete lifespan data are available in Supplementary Table 10.

RNA interference. All RNAi constructs came from the Ahringer RNAi library, except *hrp-2* and *hrpf-1* RNAi constructs, which originated from the Vidal RNAi library. RNAi experiments were carried out using *E.coli* HT115 bacteria on standard NGM plates containing 100 µg ml^{-1} carbenicillin. HT115 bacteria expressing RNAi constructs were grown overnight in LB supplemented with 100 µg ml^{-1} carbenicillin and 12.5 µg ml^{-1} tetracycline. NGM plus carbenicillin plates were seeded 48 h before use. Respective dsRNA expressing HT115 bacteria were induced by adding 100 µl IPTG (100 mM) one hour before introducing worms to the plate. RNAi was induced from egg hatch unless otherwise noted. 'ev' denotes empty vector HT115 RNAi bacteria. All verified sequences of RNAi clones are listed in Supplementary Data 1.

Solid plate-based dietary restriction assays. sDR assays were performed as described by Ching *et al.*[16]. Plates were prepared in advance and stored at 4 °C. 5-Fluoro-2′-deoxyuridine (FUDR) was added on top of the bacterial lawn (100 µl of 1 mg ml^{-1} solution in M9) 24 h before worms were introduced to the plates for lifespans or directly into the NGM at 25 µM concentration for imaging experiments. *Ad libitum* (AL) plates were prepared with a bacterial concentration of 10^{11} c.f.u. per ml and dietary restriction plates with 10^{8} c.f.u. per ml bacterial concentration.

Imaging. Worms were anaesthetized in 0.1 mg ml^{-1} tetramisole/M9 on an NGM plate without bacteria until no movement was detectable, aligned to groups accordingly and subsequently imaged on a Zeiss Discovery V8 microscope with Axiocam camera. Single worms were imaged on Zeiss Imager.M2 with 10× magnification. Exposure times were kept constant for all imaging experiments involving the splicing reporter. Worm population size was >50 worms per experiment and images represent population phenotype. Representative images were processed with ImageJ. Pixel intensity was determined per worm for EGFP and mCherry and background fluorescence subtracted from the mean intensity to calculate corrected total worm fluorescence (CTWF) = integrated density – (area of selected worm × mean fluorescence of background readings). Results were graphed using Graphpad Prism 6. All imaging experiments were repeated.

Pumping rates. Wild-type and *eat-2(ad1116)* worms were synchronized by timed egg lay onto empty vector (control) and *sfa-1* dsRNA-expressing HT115. Day 1 adult worms were transferred onto control and RNAi plates with FUDR. Pumping rates were assayed 7 h after transfer and on day 4 of adulthood. Pumps of the terminal pharyngeal bulb were counted for 1 min intervals per worm crawling on the bacterial lawn. Pumping rates per minute for ten worms per treatment were averaged. Pumping rates were assessed in two independent replicate experiments.

SFA-1 overexpression. SFA-1 is N-terminally tagged with 3× FLAG and cDNA was constructed using two gBlock gene fragments (IDT) and Gibson assembly protocol (NEB, according to the manufacturer's protocol). *sfa-1* cDNA expression is driven by *eft-3* promoter and the cDNA insertion was verified by sequencing. The plasmid was injected at 15 ng µl^{-1} concentration into N2 worms using a *myo-2p::tdTomato* expressing plasmid as co-injection marker. Lines are denoted SFA-1 OE line 1 and SFA-1 OE line 2. Additional lines were made by co-injection of 10 ng µl^{-1} *sfa-1* cDNA plasmid and *myo-3p::mCherry* into N2 worms. These lines are named SFA-1 OE line 3 and SFA-1 OE line 4.

RNA isolation and cDNA synthesis. Total RNA was extracted using Qiazol reagent (QIAGEN), column purified by RNeasy mini or miRNeasy micro kit (QIAGEN) according to the manufacturer's instructions. cDNA was synthesized using SuperScript VILO Master mix (Invitrogen).

Ageing/dietary reaction RNA sequencing sample preparation. Wild-type (N2) and *eat-2(ad1116)* (dietary restricted) worms were synchronized on HT115 empty vector (ev) or *sfa-1* RNAi bacteria by egg lay. Worms were transferred to FUDR-treated bacteria plates on day 1 of adulthood. All worms were transferred at day 3 of adulthood to fresh plates with respective FUDR-treated RNAi bacteria. Wild-type and dietary restricted worms on empty vector and *sfa-1* RNAi bacteria were collected in M9 buffer and frozen in Qiazol (QIAGEN) for RNA isolation. At day 15 of adulthood, remaining live worms were transferred to fresh plates to remove dead worms before collection in Qiazol and storage at −80 °C until RNA extraction. On day 27, live dietary restricted worms were transferred to fresh plates and frozen in Qiazol. At least 500 worms were collected for each sample at the different time points. RNA extractions were performed with two replicate sets at a time using RNeasy Mini kit (QIAGEN). RNA concentrations and quality were determined by Nanodrop and by Agilent Bioanalyzer 2100 (Agilent Technologies). Only RNA samples with RIN >8.0 were used for library preparation. RNA samples were further processed at the Harvard Biopolymers Facility. cDNA was synthesized using SMART-Seq v4 Ultra Low Input RNA kit (Clontech Laboratories). cDNA quality and concentration was assessed on Agilent 2100 Bioanalyzer before proceeding to library preparation using Nextera XT DNA library protocol (Illumina). Library quality control was performed on 2200 High Sensitivity D1000 Tape Station (Agilent Technologies). Libraries were pooled to a concentration of 1 nM and run on an Illumina HiSeq2500 with 100-cycle paired-end sequencing. Sequencing was done with four biological replicate populations for each time point.

***hrp-2* knockdown RNA sequencing.** The temperature-sensitive sterile *glp-4(bn2)* mutant strain was used for RNA-seq and the experiment was performed with three biological replicates. Worms were grown to gravid adults and bleached to collect staged eggs. Eggs were pipetted on to IPTG-induced NGM plus carbenicillin plates prepared with either empty vector (ev) HT115 or *hrp-2* dsRNA expressing bacteria. Worms were grown at 15 °C for 24 h, then shifted to 22.5 °C to prevent normal proliferation of germ cells and progeny development. Day 1 adult worms were washed off empty vector and *hrp-2* plates in M9 following snap freeze in Qiazol (QIAGEN) for RNA extraction. RNA extraction was performed in parallel for two replicates with a third replicate added later to obtain similar RNA levels. RNA extractions were done according to the manufacturer's protocol using RNeasy mini kit (QIAGEN). RNA quality was confirmed on Agilent 2100 Bioanalyzer and all samples had RIN >8.6. cDNA libraries were prepared from 1 µg total RNA using TruSeq RNA Sample preparation v2 kit (Illumina). 100-cycle paired-end sequencing was performed on HiSeq 2500 (Illumina) by the Tufts University Core Facility.

SF1 knockdown in HeLa cells and RNA sequencing sample preparation. HeLa cells were grown in RPMI1640 supplemented with 10% fetal calf serum (FCS), glutamine and penicillin/streptomycin (HeLa EMBL cells: Provided by the Eugene laboratory at University of Southern Denmark; cells were authenticated by confirming 93% SNPs listed in COSMIC database; not tested for mycoplasma contamination). The cells were reverse transfected using RNAiMAX (ThermoFisher Scientific) and siRNAs targeting SF1 (L-012662-01-0020, Dharmacon) or non-targeting siRNAs (D-001810-10-20) as control. After 24 h, cells were re-transfected using the forward transfection protocol and 48 h later harvested for RNA and protein. Knockdown of SF1 was validated by western blotting. Total RNA was isolated using Isol-RNA lysis reagent (5 PRIME). RNA purity, integrity and concentration were determined using an Agilent 2100 Bioanalyzer (Agilent Technologies). Only RNA samples with a RIN value of 8.0 or higher and a ratio (28 s/18 s) of above 1.8 were used in sequencing library preparation. Three biological replicates for control and SF1 knockdown samples were processed for library constructions following the manufactory instructions (Illumina Tru Seq Stranded Total RNA sample preparation v2 Guide, Part #15031048 Rev.E October 2013 – Low sample protocol). In brief, 0.5 µg of total

RNA from each tissue was depleted for cytoplasmic rRNA using the Ribo-Zero ribosomal reduction chemistry, chemically fragmented for 8 min at 94 °C, and processed for 1st strand synthesis cDNA and then 2nd strand synthesis using dUTP instead of dTTP. After some purification steps, the cDNA was then end-repaired, purified, adenylated at the 3′-ends, and purified before adding the indexed adaptor sequences using the TruSeq Stranded LT Kit Index set A. Each library preparation was then enriched by ten cycles of PCR, purified and finally validated in regards to size and concentration. For sizing, libraries were analysed on the Agilent 2100 Bioanalyzer using a DNA 1000 kit from Agilent Technologies. The libraries were quantified by qPCR using the KaPa Library quantification Kits (KaPa Biosystems, Cat KK4824). Samples were pooled, and a final concentration of 16 pM denatured library was used for 100-cycle paired-end sequencing using an Illumina HiSeq1500 at the University of Southern Denmark's Villum Center for Bioanalytical Sciences.

RNA sequencing analysis. Raw reads were adaptor trimmed with cutadapt[31] using the additional parameters '–trim-n -m 15' and subsequently aligned to WBcel235 and hg38 genomes with STAR[32] version 2.5.0c using the additional parameter '–alignIntronMax 50000' for the WBcel235 alignments and the additional parameters '–outSAMstrandField intronMotif–outFilterType BySJout' for all alignments. Gene counts were obtained with htseq-count[33] and WBcel235 Ensembl annotation v75 (ref. 34) and hg38 Ensembl annotation v79. Gene expression analysis was performed using DESeq2 (ref. 35) with cqn-based[36] normalization. After adjusting for multiple testing using the Benjamini–Hochberg method[37], we defined differentially expressed genes as those with adjusted *P* values (*q* value) below 0.1. GO term enrichment analysis of differentially expressed genes was carried out using goseq[38] and KEGG pathway analysis with gage[39], significantly altered pathways and GO terms were defined as having Benjamini–Hochberg-adjusted *P* values (*q* values) below 0.1. Overall KEGG pathway activity was estimated by averaging the regularized log-transformed expression estimates from each sample over each condition. Splicing analysis was performed with SAJR[40] by first constructing *de novo* annotation from the Ensembl input and merged alignment files. Inclusion and exclusion reads were subsequently obtained for each splicing event and analysed using a GLM model under a quasibinomial distribution. Before model parameter estimation we restricted the analysis to only those splicing events for which we could map at least five inclusion reads and five exclusion reads across conditions. Significant splicing changes were defined as those with *P* values below 0.05 after adjusting for multiple testing using Benjamini–Hochberg correction. PTC containing regions were defined as those containing a stop-codon in all possible reading frames at least 50 bp upstream of the next downstream splicing site.

GO term enrichment analysis on genes with increased intron retention was performed with goseq and limited to terms for which we had at least two genes with increased intron retention. KEGG pathway enrichment analysis was performed with clusterProfiler[41] with a background set of all Entrez IDs mapped to a KEGG pathway.

Ageing/RAGA-1 mutant sample collection. Wild-type (N2) and *raga-1(ok386)* worms were grown and collected following the same procedure as described above for ageing/dietary restriction sample collection.

Semi-quantitative RT–PCR of alternative splicing events. *tos-1* was amplified using modified PCR conditions and full-length *tos-1* cDNA primers according to ref. 20. Expand High Fidelity PCR System (Roche) or Apex Taq RED (Genesee Scientific) was used for amplification with an annealing temperature of 60 °C and 35 cycles.

Alternative splicing events detected by our RNA-seq analysis were validated using Apex Taq RED master mix. 1 kb Plus DNA ladder (Invitrogen) was used as molecular weight reference. Following PCR, samples were resolved on a 2% agarose gel and stained with ethidium bromide. Gels were imaged on ChemiDoc MP (BioRad). All reactions were run with a minimum of two biological replicate samples. Primer sequences are provided in Supplementary Data 2.

Quantitative RT–PCR. Taqman real-time qPCR experiments were performed on a StepOne Plus instrument (Applied Biosystems) following the manufacturer's instructions. Data were analysed with the comparative $2^{\Delta\Delta C_t}$ method using *Y45F10D.4* (Ce02467253_g1) as endogenous control. For each gene in each strain, average fold-change relative to the wild type was calculated and statistical significance evaluated with a one-way analysis of variance (ANOVA). The following Taqman assays from Life Technologies were used: *sfa-1* (Ce02468921_m1), *uaf-2* (custom made), *rsr-2* (Ce02439948_g1), *cpr-1* (Ce02482188_g1), *acs-2* (Ce02486192_g1), *acs-17* (Ce02495808_g1), *fat-5* (Ce02488494_m1), *fat-6* (Ce02465318_g1), *fat-7* (Ce02477067_g1), *acdh-2* (Ce02432818_g1), *lips-17* (Ce02435133_g1) and *gst-4* (Ce02458730_g1).

EGFP and mCherry expression analysis was performed using Fast SYBR Green Master Mix (Applied Biosystems) on a StepOne Plus instrument (Applied Biosystems) according to the manufacturer's instructions. A standard curve was prepared to analyse EGFP and mCherry primer efficiencies. Data were analysed with the comparative $2^{\Delta\Delta C_t}$method using *Y45F10D.4* and *pmp-3* mRNA levels as endogenous controls. Graphpad Prism 6 was used for all statistical analysis.

Oxygen consumption. N2 and *eat-2(ad1116)* worms were grown on empty vector or *sfa-1* RNAi bacteria from egg hatch. Worms were transferred to plates with FUDR on day 1 of adulthood. Oxygen consumption was measured on day 4 and day 15 of adulthood using a Seahorse XF96 analyser (Seahorse Bioscience). Worms were removed from NGM plates, washed 3 times with M9 buffer and transferred to a 96-well plate (10 worms per well). Basal respiration was measured ten times followed by the addition of FCCP (10 μM) to measure maximal respiration, which was measured six times. Oxygen consumption rates were normalized to the number of worms per well. Two biological replicate experiments were run.

SF1 knockdown in mouse embryonic fibroblast (MEF) cells and immunoblotting. Wild-type MEFs were maintained in Dulbecco's Modified Eagle's Medium (DMEM; Corning/Cellgro, 10-017-CV) containing 10% fetal bovine serum (FBS) (Proven to be mycoplasma contamination negative; cell line identified by qRT–PCR and western blot (Manning laboratory); Wild-type MEFs were provided by the laboratory of D. Kwiatkowski. Wild-type MEFs were serum starved for 16 h, pre-treated with rapamycin (20 nM) or torin (250 nM) for 30 min before insulin stimulation (1 h and 16 h, 500 nM). To control for the SF1 antibody specificity, Wild-type MEFs were transfected with non-targeting control siRNAs (siCt) or SF1 siRNA for 72 h and grown in 10% FBS. Cells were lysed in ice-cold Triton lysis buffer (40 mM HEPES, pH 7.4, 120 mM NaCl, 1 mM EDTA, 1% Triton X-100, 10 mM sodium pyrophosphate, 10 mM glycerol 2-phosphate, 50 mM NaF, 0.5 mM sodium orthovanadate, 1 μM Microcystin-LR, 0.2 mM PMSF and protease inhibitor cocktail). Lysates were clarified by centrifugation (20,000*g* for 15 min at 4 °C) and protein concentrations were determined using the Bradford assay (Biorad). Normalized protein lysates were loaded onto 8% acrylamide resolving gels, separated by SDS–PAGE, transferred to nitrocellulose membranes and subjected to immunoblotting with the indicated antibodies. siRNA against mouse SF1 was from Sigma (cat no. SASI_Mm02_00305738) and non-targeting control siRNA was from Dharmacon. Antibodies towards SF1 (cat no. HPA018883-100UL) and β-actin were from Sigma. Phospho (P)-S6K1 T389 (CST #9234), phospho (P)-S6 S240/S244 (CST #2215), S6K1 (CST #2708) and S6 (CST #2217) were from Cell Signaling technologies. These experiments were repeated twice.

Phospho-S6K immunoblotting. For each sample, approximately 500 day 1 adult *C. elegans* were collected in M9 buffer and snap-frozen in liquid nitrogen. To make worm lysates, RIPA buffer with protease inhibitors (Sigma #8340) and phosphatase inhibitors (Roche #4906845001) were added and samples were lysed via sonication (Qsonica Q700). SDS–PAGE were performed using 10% Tris-glycine gels (Thermo Fisher Scientific, #XP00100). Proteins were transferred to PVDF membranes (Thermo Fisher Scientific, #LC2005) and blocked with 5% BSA in TBST. Primary antibodies and dilutions are: phospho-*Drosophila* p70 S6 kinase (Thr398) (Cell Signaling, #9209, 1:500), β-actin (Abcam, #8226, 1:1000). Bands were visualized and quantified using a Gel Doc system (Bio Rad) and Image Laboratory software (Version 4.1).

Code availability. Computer code will be deposited in Protocol Exchange repository.

Data availability. All RNA-seq datasets generated and analysed during the current study are available in the ArrayExpress Archive with the accession number E-MTAB-4866. All other data are available from the corresponding author upon reasonable request.

29. Mair, W. *et al.* Lifespan extension induced by AMPK and calcineurin is mediated by CRTC-1 and CREB. *Nature* **470,** 404–408 (2011).
30. Burkewitz, K. *et al.* Neuronal CRTC-1 governs systemic mitochondrial metabolism and lifespan via a catecholamine signal. *Cell* **160,** 842–855 (2015).
31. Martin, M. Cutadapt removes adapter sequences from high-throughput sequencing reads. *EMBnet.journal* **17,** 10–12 (2011).
32. Dobin, A. *et al.* STAR: ultrafast universal RNA-seq aligner. *Bioinformatics* **29,** 15–21 (2013).
33. Anders, S., Pyl, P. T. & Huber, W. HTSeq--a Python framework to work with high-throughput sequencing data. *Bioinformatics* **31,** 166–169 (2015).
34. Cunningham, F. *et al.* Ensembl 2015. *Nucleic Acids Res.* **43,** D662–D669 (2015).
35. Love, M. I., Huber, W. & Anders, S. Moderated estimation of fold change and dispersion for RNA-seq data with DESeq2. *Genome Biol.* **15,** 550 (2014).
36. Hansen, K. D., Irizarry, R. A. & Wu, Z. Removing technical variability in RNA-seq data using conditional quantile normalization. *Biostatistics* **13,** 204–216 (2012).
37. Benjamini, Y. & Hochberg, Y. Controlling the false discovery rate: a practical and powerful approach to multiple testing. *J. R. Stat. Soc. B* **57,** 289–300 (1995).
38. Young, M. D., Wakefield, M. J., Smyth, G. K. & Oshlack, A. Gene ontology analysis for RNA-seq: accounting for selection bias. *Genome Biol.* **11,** R14 (2010).
39. Luo, W., Friedman, M. S., Shedden, K., Hankenson, K. D. & Woolf, P. J. GAGE: generally applicable gene set enrichment for pathway analysis. *BMC Bioinformatics* **10,** 161 (2009).
40. Mazin, P. *et al.* Widespread splicing changes in human brain development and aging. *Mol. Syst. Biol.* **9,** 633–633 (2013).
41. Yu, G., Wang, L. G., Han, Y. & He, Q. Y. clusterProfiler: an R package for comparing biological themes among gene clusters. *OMICS* **16,** 284–287 (2012).

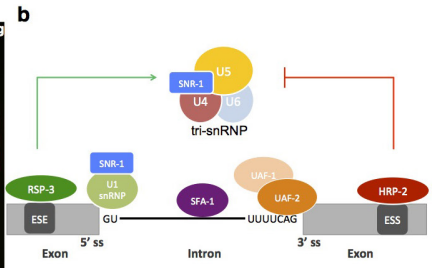

c

C. elegans gene name	Mammalian protein homologue	Name	Function
uaf-2	U2AF35	U2 auxiliary factor small subunit	Core spliceosomal factor
uaf-1	U2AF65	U2 auxiliary factor large subunit	Core spliceosomal factor
sfa-1	SF1/BBP	Splicing factor 1, branch point binding protein	Core spliceosomal factor
repo-1	SF3A2	Splicing factor 3a subunit 2 (66kDa)	Core spliceosomal factor
snr-1	SNRPD3	Small nuclear ribonucleoprotein Sm D3	Core spliceosomal factor
snr-2	SNRPB	Small nuclear ribonucleoprotein Sm B	Core spliceosomal factor
rsp-2	SRSF5, SRp40	Serine/Arginine-rich splicing factor 5	Extrinsic non spliceosomal RNA binding protein
rsp-3	SRSF1, SF2/ASF	Serine/Arginine-rich splicing factor 1	Extrinsic non spliceosomal RNA binding protein
hrp-1	hnRNP A1	Heterogeneous nuclear ribonucleoprotein A1	Extrinsic non spliceosomal RNA binding protein
hrp-2	hnRNP R	Heterogeneous nuclear ribonucleoprotein R	Extrinsic non spliceosomal RNA binding protein
hrpf-1	hnRNP F/H	Heterogeneous nuclear ribonucleoprotein F/H	Extrinsic non spliceosomal RNA binding protein
prp-8	PRPF8	Pre-mRNA processing splicing factor 8	Core spliceosomal factor
phi-9	NHP2L1	NHP2-like protein 1	RNA binding protein
smu-1	SMU1	WD40 repeat-containing protein SMU1, fSAP57	RNA binding protein
sym-2	hnRNP F/H	Heterogeneous nuclear ribonucleoprotein F/H	Extrinsic non spliceosomal RNA binding protein

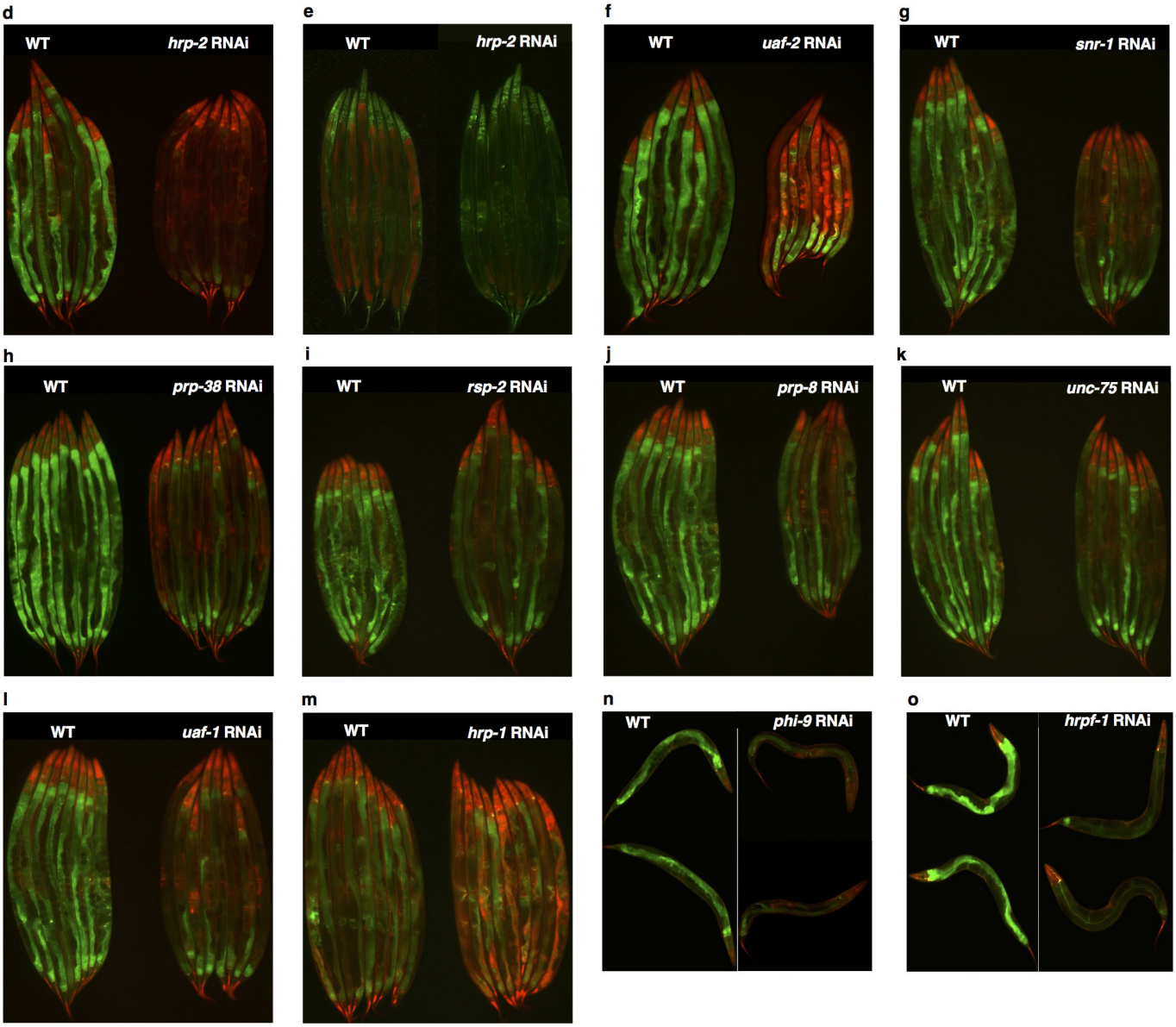

Extended Data Figure 1 | Heterogeneous splicing patterns in response to knockdown of conserved splicing factors. a, Inverted fluorophore splicing reporter. **b**, Simplified diagram of *C. elegans* intron splicing showing representative splicing factors investigated herein **c**, *C. elegans* splicing factors and their mammalian homologues. **d**–**l**, Knockdown of *hrp-2* in splicing reporter (**d**) and *hrp-2* in inverted reporter (**e**), *uaf-2* (**f**), *snr-1* (**g**), *prp-38* (**h**), *rsp-2* (**i**), *prp-8* (**j**), *unc-75* (**k**) and *uaf-1* (**l**) by RNAi at day 1 of adulthood. **m**, *hrp-1* depletion at day 4 of adulthood. **n**, **o**, Representative images of worms with *phi-9* (**n**) and *hrpf-1* (**o**) knockdown in day 1 adults with reduced exon inclusion.

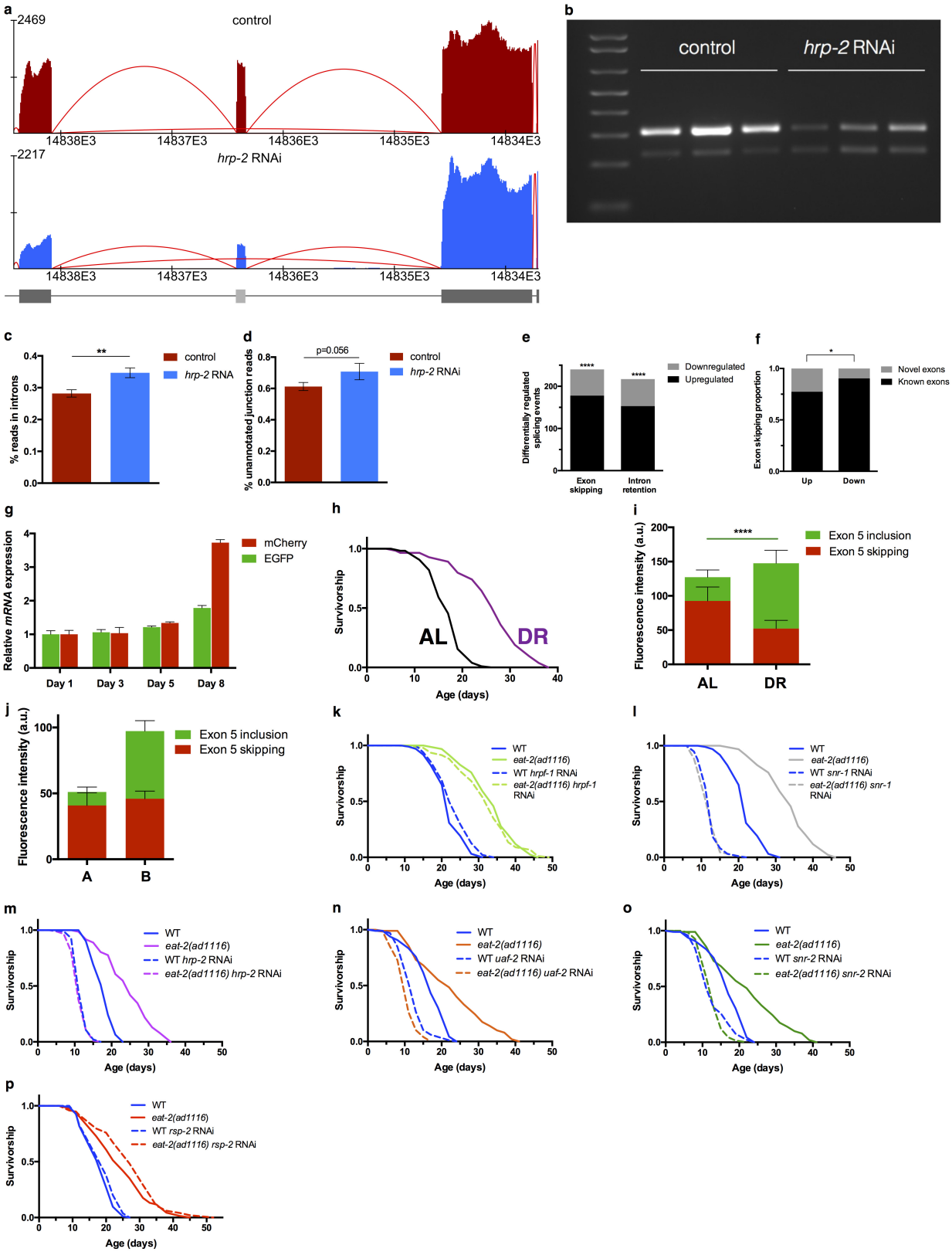

Extended Data Figure 2 | See next page for caption.

Extended Data Figure 2 | Effects of splicing factor knockdown on splicing homeostasis and dietary-restriction-mediated longevity. **a**, RNA-seq coverage tracks for endogenous *ret-1* splicing in *hrp-2* knockdown samples. Sequencing reads tracks generated by Splicing Java Coverage Viewer as part of SAJR[40]. Height of red lines represents RNA coverage of splice junctions, dark grey boxes represent exonic sequence, light grey box denotes alternative exon sequence. **b**, Endogenous *ret-1* splicing exon 5 skipping in wild-type and *hrp-2* RNAi worms by RT–PCR (three biological replicates). **c**, **d**, Intronic reads (**c**, $P = 0.0042$) and unannotated junctions reads (**d**, $P = 0.056$) as hallmarks of deregulated splicing with *hrp-2* knockdown. Three biological replicates for control and with *hrp-2* RNAi. Mean ± s.e.m., per cent of total reads shown. *P* values calculated with unpaired, two-tailed *t*-test after probit transformation. **e**, Differentially regulated alternative splicing events induced by *hrp-2* depletion (****$P < 0.0001$ for exon inclusion, intron retention $P < 0.0001$, Pearson's χ^2 test). **f**, Proportion plot of all exon skipping events with proportions of novel and known exons up- or downregulated in *hrp-2* knockdown samples (*$P = 0.0157$, differences in proportions of novel exons in up- and downregulated events were tested with Pearson's χ^2 test, deviations from an even proportion of up- and downregulated splicing events were tested with binomial test). **g**, EGFP and mCherry mRNA levels up to day 8 of adulthood by qRT–PCR (mean + s.d., technical replicates shown, 1 of 2 biological replicates). **h**, sDR robustly extends the lifespan of *C. elegans* fed *ad libitum*[16] ($P < 0.0001$). **i**, Fluorescence quantification of splice isoforms in 7-day-old *ad libitum* and sDR animals (****$P < 0.0001$, unpaired two-tailed *t*-test, mean + s.d., $n = 8$ worms per condition, 6 biological replicates). **j**, Age-matched, *ad libitum*-fed worm populations separated at day 6 according to group A (increased exon 5 skipping) and group B (increased exon 5 inclusion) (mean + s.d., $n = 6$, 1 of 3 biological replicates shown). **k**, Effect of *hrpf-1* RNAi on wild-type and *eat-2(ad1116)* lifespan (wild-type versus *eat-2(ad1116)* with *hrpf-1* RNAi, $P < 0.0001$). **l**, Comparison of survival rates of wild-type and *eat-2(ad1116)* with *snr-1* RNAi ($P = 0.5147$). **m**, **n**, Survival analysis of *hrp-2* (**m**) and *uaf-2* (**n**) downregulation by RNAi (wild-type with *hrp-2* RNAi versus *eat-2(ad1116)* with *hrp-2* RNAi, $P = 0.1617$, 2 replicates; wild-type with *uaf-2* RNAi versus *eat-2(ad1116)* with *uaf-2* RNAi, $P = 0.001$, 3 replicates). **o**, Effect of *snr-2* knockdown on wild-type and dietary-restricted lifespan (wild-type with *snr-2* RNAi versus *eat-2(ad1116)* with *snr-2* RNAi, $P = 0.3456$, 2 replicates). **p**, Wild-type and dietary-restricted lifespan curves with *rsp-2* knockdown (wild-type with *rsp-2* RNAi versus *eat-2(ad1116)* with *rsp-2* RNAi, $P < 0.0001$, 3 replicates). Lifespan experiments done with FUDR as indicated in Extended Data Table 1 and Supplementary Table 10. $n = 100$ worms per condition for lifespan analysis. *P* values of survival analysis calculated with log-rank test.

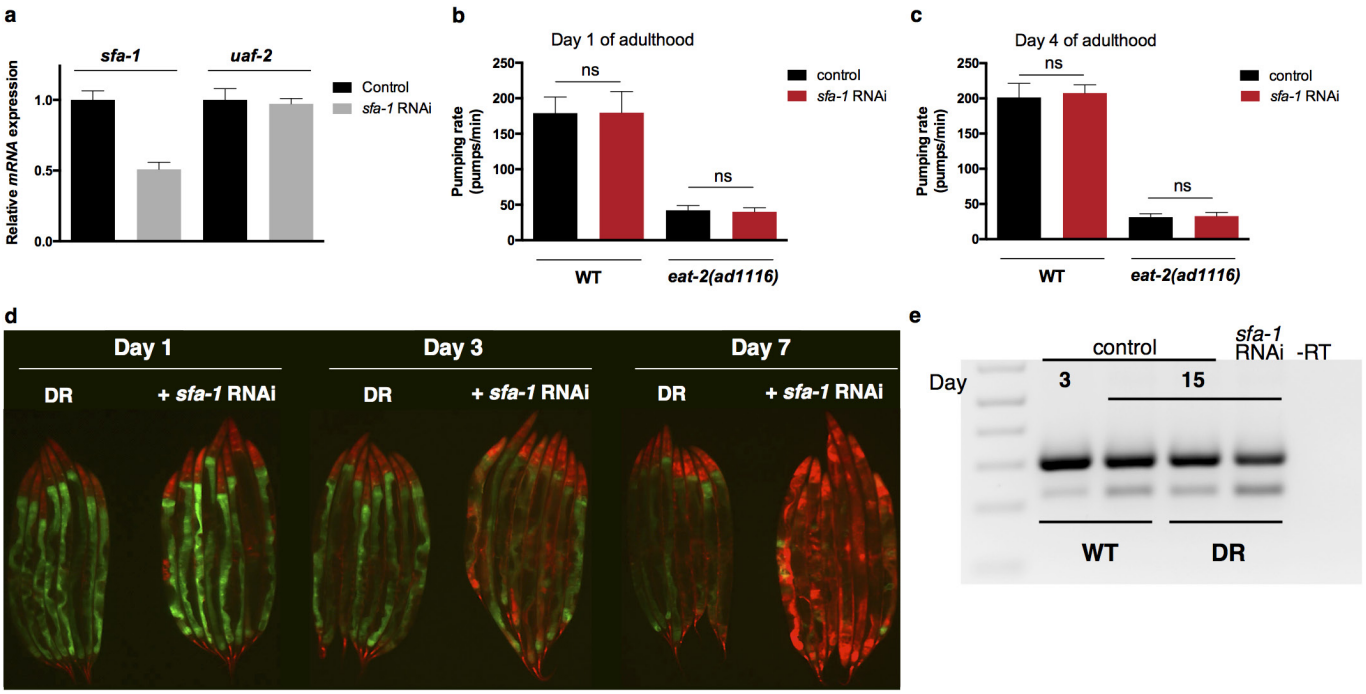

Extended Data Figure 3 | Effects of *sfa-1* downregulation on splicing. **a**, Expression of *uaf-2* is not affected by reduced *sfa-1* levels in wild-type worms at day 1 of adulthood (mean + s.d., technical replicates shown). **b**, **c**, Effect of reduced *sfa-1* expression on pumping rates in wild-type and a genetic dietary restriction model (*eat-2(ad1116)*) at day 1 (**b**) and 4 of adulthood (**c**) (mean + s.d., ns, $P > 0.05$, unpaired, two-tailed *t*-test, $n = 10$ worms per condition, 1 of 2 replicates shown). **d**, Splicing reporter pattern with *sfa-1* knockdown from egg hatch, day 1, 3 and 7 adults. **e**, Endogenous *ret-1* exon 5 splicing pattern with age and *sfa-1* RNAi in wild-type and dietary-restricted worms by RT–PCR (day 3 versus 15, fifth replicate sample set).

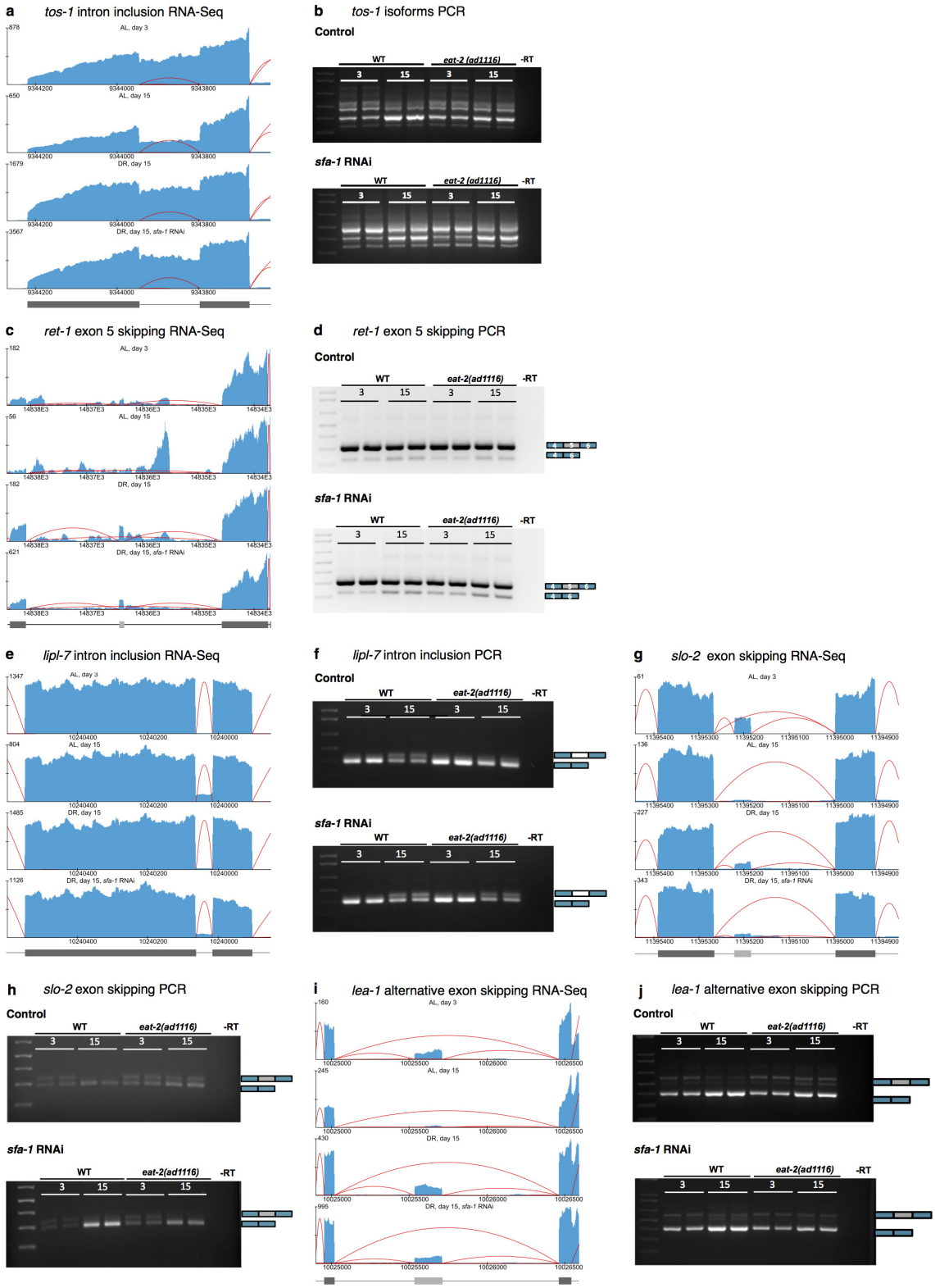

Extended Data Figure 4 | RT–PCR validation of alternative splicing events in ageing and with *sfa-1* knockdown. a, Sequencing reads coverage for *tos-1* **b**, Age-associated isoform ratio change of a target of SFA-1, *tos-1*, in wild-type worms at day 3 and 15 of adulthood with or without *sfa-1* RNAi by RT–PCR (two biological replicates, distinct from those used in Fig. 1i, shown). **c**, Sequencing read coverage map for *ret-1* shows increased exon 5 skipping with age and with *sfa-1* RNAi. **d**, Endogenous *ret-1* exon 5 splicing pattern with age and *sfa-1* RNAi in wild-type and dietary-restricted worms by RT–PCR (day 3 versus 15, two biological replicates shown). **e**, Sequencing tracks for *lipl-7* pre-mRNA. **f**, Monitoring of intron retention between exons 4 and 5 at day 15 versus day 3 of adulthood in wild-type and dietary-restricted worms with or without *sfa-1* RNAi. **g**, Sequencing reads tracks for *slo-2* pre-mRNA. **h**, *slo-2* alternative exon skipping in day 3 and day 15 wild-type and dietary-restricted worms with or without *sfa-1* RNAi. **i**, Sequencing reads tracks for *lea-1* pre-mRNA **j**, Alternative exon skipping in *lea-1* with age and *sfa-1* knockdown in wild-type and dietary-restricted animals. Two biological replicates shown for all RT–PCR analyses. Sequencing reads tracks generated by Splicing Java Coverage Viewer as part of SAJR[40]; height of red lines represent RNA coverage of splice junctions, dark grey boxes represent exonic sequence, light grey boxes denote the alternative exon sequence.

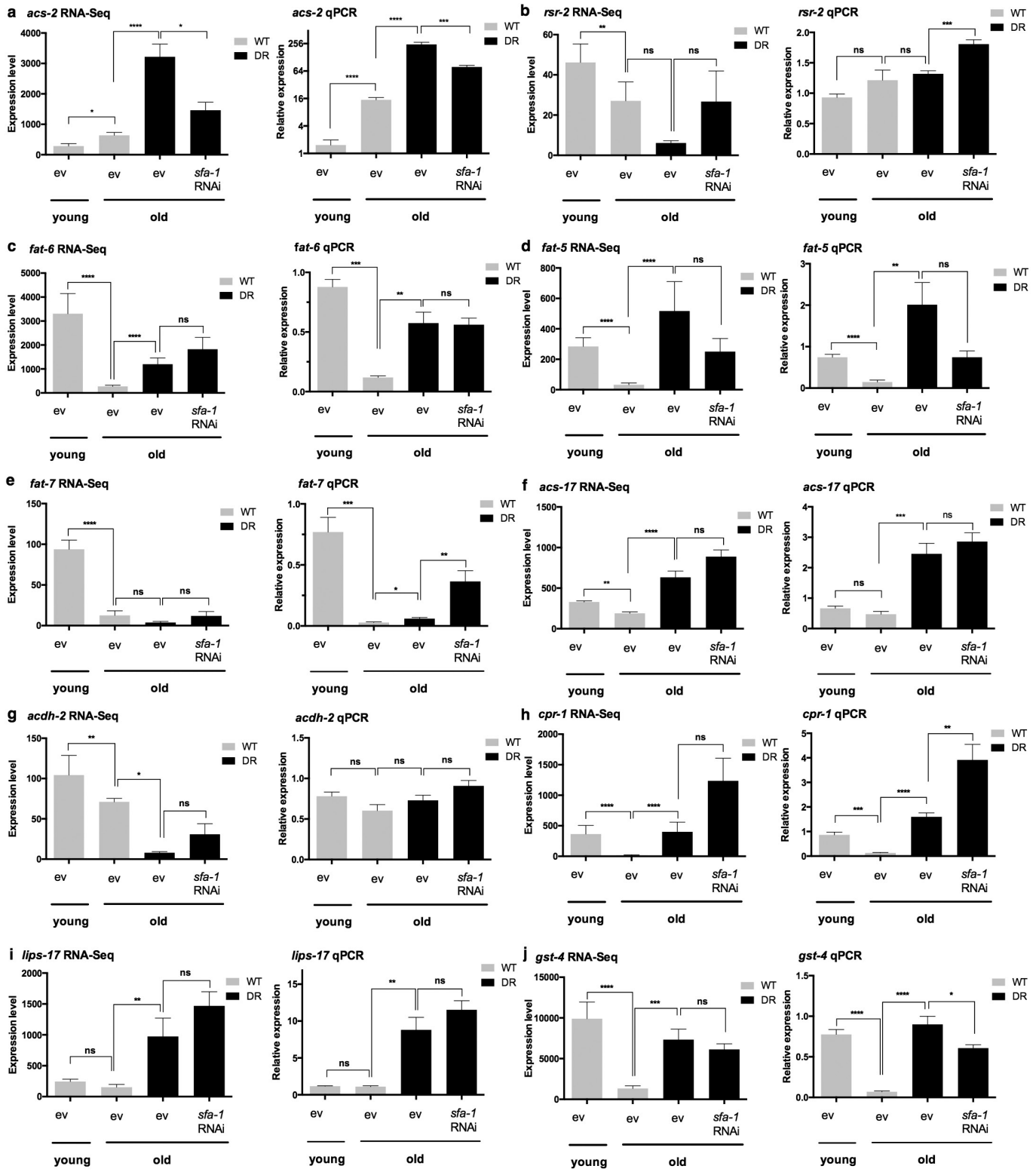

Extended Data Figure 5 | RNA-seq expression data validation by quantitative RT–PCR. a–j, Monitoring of gene expression levels by quantitative RT–PCR for RNA-seq data validation of *acs-2* (**a**), *rsr-2* (**b**), *fat-6* (**c**), *fat-5* (**d**), *fat-7* (**e**), *acs-17* (**f**), *acdh-2* (**g**), *cpr-1* (**h**), *lips-17* (**i**) and *gst-4* (**j**) in 6 biological replicates for 3-day-old wild-type worms and 5 biological replicates for all other samples at day 15 (****$P \leq 0.0001$, ***$P \leq 0.001$, **$P \leq 0.01$, *$P \leq 0.05$; ns, $P > 0.05$; RNA-seq data are mean + s.e.m. of normalized read counts of 4 biological replicates. qRT–PCR data are mean + s.e.m. *P* values calculated with unpaired, two-tailed *t*-test).

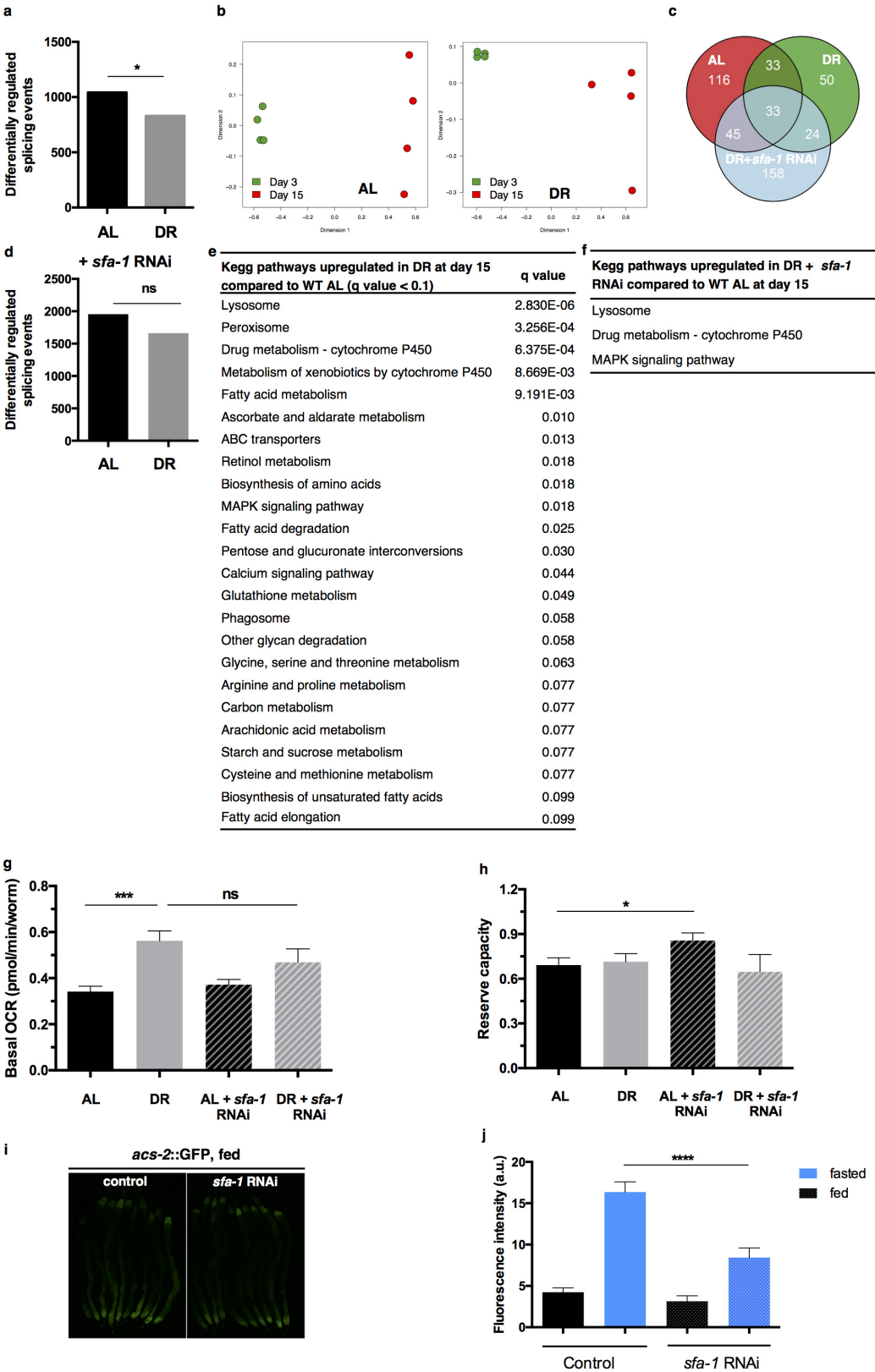

Kegg pathways upregulated in DR at day 15 compared to WT AL (q value < 0.1)	q value
Lysosome	2.830E-06
Peroxisome	3.256E-04
Drug metabolism - cytochrome P450	6.375E-04
Metabolism of xenobiotics by cytochrome P450	8.669E-03
Fatty acid metabolism	9.191E-03
Ascorbate and aldarate metabolism	0.010
ABC transporters	0.013
Retinol metabolism	0.018
Biosynthesis of amino acids	0.018
MAPK signaling pathway	0.018
Fatty acid degradation	0.025
Pentose and glucuronate interconversions	0.030
Calcium signaling pathway	0.044
Glutathione metabolism	0.049
Phagosome	0.058
Other glycan degradation	0.058
Glycine, serine and threonine metabolism	0.063
Arginine and proline metabolism	0.077
Carbon metabolism	0.077
Arachidonic acid metabolism	0.077
Starch and sucrose metabolism	0.077
Cysteine and methionine metabolism	0.077
Biosynthesis of unsaturated fatty acids	0.099
Fatty acid elongation	0.099

Kegg pathways upregulated in DR + *sfa-1* RNAi compared to WT AL at day 15	q value
Lysosome	0.0152
Drug metabolism - cytochrome P450	0.0450
MAPK signaling pathway	0.0450

Extended Data Figure 6 | See next page for caption.

Extended Data Figure 6 | Genome-wide effects of dietary restriction and SFA-1 depletion on pre-mRNA splicing and metabolism. **a**, Differentially regulated splicing events (exons, introns, alternative 5′ and 3′ splice sites) in dietary restriction at day 15 compared to feeding *ad libitum* (*$P = 0.0156$, Wilcoxon signed rank test). **b**, Multidimensional scaling plot of significantly different splicing patterns using inclusion ratio estimates between day 3 and day 15 worms (changes in all significant pre-mRNA segments, for example, exons, introns, alternative splice sites, considered). **c**, Venn diagram representing significantly up- or downregulated novel splicing events at day 15 in worms fed *ad libitum*, worms on dietary restriction and dietary restriction with *sfa-1* RNAi (subset of unannotated splice junctions). **d**, Differentially regulated splicing events (exons, introns, alternative 5′ and 3′ splice sites) with *sfa-1* knockdown (*ad libitum* with *sfa-1* RNAi versus dietary restriction with *sfa-1* RNAi, $P = 0.7999$, Wilcoxon signed rank test). **e**, KEGG pathways significantly upregulated in dietary-restricted worm populations at day 15 compared to wild-type worm populations of the same chronological age with false discovery rate (FDR) of 10%. **f**, KEGG pathways significantly upregulated in dietary-restricted worm populations with *sfa-1* knockdown at day 15 compared to worm populations fed *ad libitum* with FDR 10%. **g**, **h**, Basal respiration (**g**) and reserve capacity (**h**) in wild-type and dietary-restricted animals (mean + s.e.m., ***$P \leq 0.001$, *$P \leq 0.05$, unpaired two-tailed *t*-test). Results shown are oxygen consumption rates of 15-day-old worms normalized to 4-day-old populations, $n = 100$ worms per condition (1 of 3 replicate experiments). **i**, Transcriptional induction of *acs-2p::GFP* in fed control and *sfa-1* knockdown worms (representative image of two repeat experiments shown, *n* worms: empty vector, fed, $n = 83$; empty vector, fasted, $n = 77$; *sfa-1* RNAi, fed, $n = 76$; *sfa-1* RNAi, fasted, $n = 84$). **j**, Quantification of *acs-2p::GFP* after 23 h of fasting and *sfa-1* knockdown (mean + s.e.m. of two replicate experiments, *n* as in **i**, $P < 0.0001$, unpaired two-tailed *t*-test).

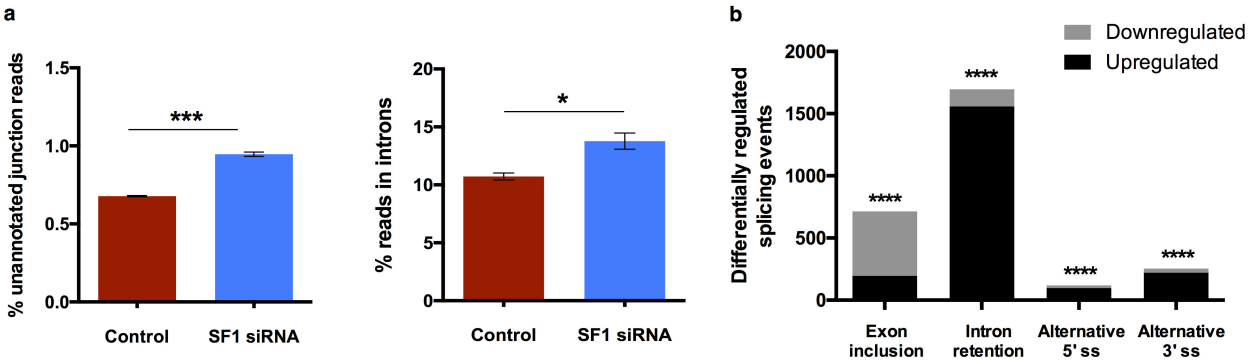

c

Kegg pathways downregulated in HeLa cells with SF1 knockdown	p value	q value
Biosynthesis of unsaturated fatty acids	0.005	0.342
Biosynthesis of amino acids	0.007	0.342
Vascular smooth muscle contraction	0.010	0.342
Carbon metabolism	0.010	0.342
Fc gamma R-mediated phagocytosis	0.016	0.342
cGMP-PKG signaling pathway	0.016	0.342
Systemic lupus erythematosus	0.016	0.342
Adrenergic signaling in cardiomyocytes	0.017	0.342
Fatty acid metabolism	0.018	0.342
Pyruvate metabolism	0.019	0.342
Alanine, aspartate and glutamate metabolism	0.020	0.342
Dopaminergic synapse	0.020	0.342
Phosphatidylinositol signaling system	0.024	0.342
Sphingolipid signaling pathway	0.024	0.342
Base excision repair	0.025	0.342
Fatty acid degradation	0.025	0.342
Glycolysis / Gluconeogenesis	0.028	0.342
AMPK signaling pathway	0.029	0.342
Asthma	0.030	0.342
Morphine addiction	0.031	0.342
Progesterone-mediated oocyte maturation	0.033	0.342
Fatty acid elongation	0.034	0.342
Melanogenesis	0.034	0.342
Long-term depression	0.036	0.342
Thyroid hormone synthesis	0.036	0.342
Citrate cycle (TCA cycle)	0.037	0.342
Aldosterone-regulated sodium reabsorption	0.037	0.342
Glyoxylate and dicarboxylate metabolism	0.039	0.342
Antigen processing and presentation	0.041	0.342
Butanoate metabolism	0.041	0.342
Valine, leucine and isoleucine degradation	0.041	0.342
DNA replication	0.042	0.342
Ras signaling pathway	0.042	0.342
Autoimmune thyroid disease	0.043	0.342
Axon guidance	0.050	0.375

Extended Data Figure 7 | Effects of SF1 knockdown in HeLa cells. **a**, Effect of SF1 knockdown in HeLa cells on unannotated junction reads (mean ± s.e.m., ***$P = 0.0006$) and reads in introns (mean ± s.e.m., *$P = 0.0242$, unpaired, two-tailed t-test after probit transformation) Three biological replicate samples. **b**, Differentially regulated alternative splicing events (exon skipping, intron retention, alternative 5′ and 3′ splice sites) with SF1 knockdown. Exons are primarily downregulated, whereas introns are significantly upregulated (**** $P < 0.0001$, Pearson χ^2 test). **c**, KEGG pathway analysis of gene expression changes upon SF1 knockdown. Pathways with $P \leq 0.05$ considered significant, P values derived by gage[39]. q values are P values adjusted for multiple testing using the Benjamini–Hochberg method[37].

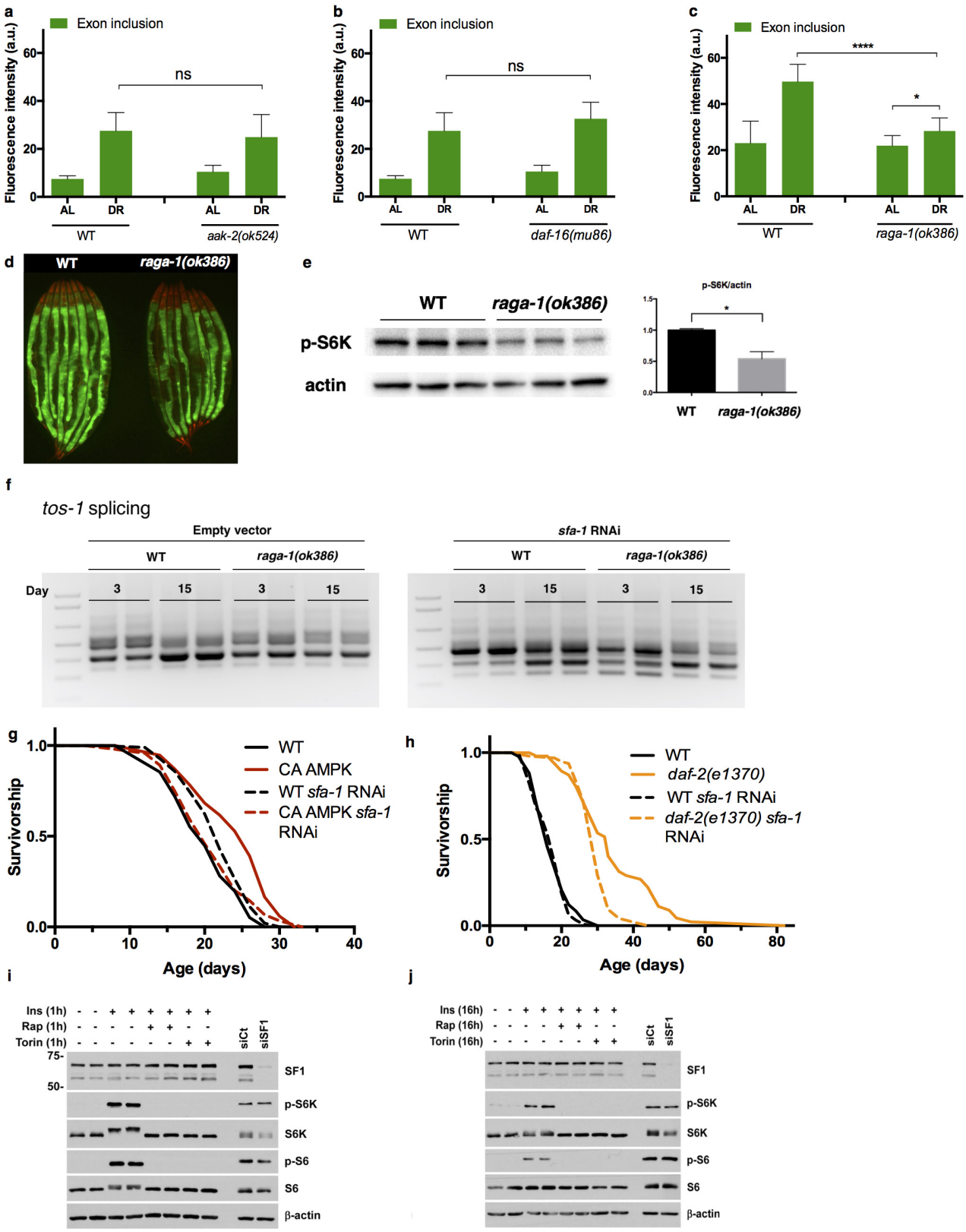

Extended Data Figure 8 | See next page for caption.

Extended Data Figure 8 | SFA-1 and the mTORC1 pathway. **a**, **b**, Quantification of *ret-1* minigene exon inclusion (GFP intensity) in *aak-2(ok524)* (**a**; *ad libitum* versus dietary restriction, $P = 0.5488$, unpaired two-tailed *t*-test, mean + s.d., $n = 8$, 3 replicates), and in *daf-16(mu86)* (**b**; *ad libitum* versus dietary restriction, $P = 0.1835$, unpaired two-tailed *t*-test, mean + s.d., $n = 8$, 2 replicates) **c**, Quantification of GFP in *raga-1(ok386)* mutants at day 8 in *ad libitum* and dietary restriction conditions (****$P < 0.0001$, *$P < 0.05$, $n = 8$, unpaired two-tailed *t*-test, mean + s.d.). One of three replicate imaging experiments shown. **d**, Splicing reporter expression in day 1 wild-type and *raga-1(ok386)* animals. **e**, Immunoblot of proteins from wild-type and *raga-1(ok386)* animals assaying S6K phosphorylation state (*$P = 0.017$, unpaired two-tailed *t*-test, mean + s.e.m., 3 biological replicates). **f**, *tos-1* isoform ratios in *raga-1(ok386)* mutants at day 3 and 15 of adulthood with *sfa-1* RNAi (2 biological replicates shown). **g**, Survival analysis of *sfa-1* RNAi in constitutively active (CA) AMPK mutant ($P = 0.4844$, wild-type with *sfa-1* RNAi versus CA AMPK with *sfa-1* RNAi). **h**, Survival analysis of SFA-1 knockdown in insulin/IGF signalling-mediated longevity (*daf-2(e1370)*, $P < 0.0001$, wild-type with *sfa-1* RNAi versus *daf-2(e1370)* with *sfa-1* RNAi. **i**, Immunoblots of proteins from wild-type mouse embryonic fibroblasts. p-S6K(T389) and p-S6(S240/S244) (assaying phosphorylation at sites T389 (S6K) and S240/S244 (S6), markers of mTORC1 activation), total S6K, total S6, non-targeting control short interfering RNAs (siCt), SF1 siRNA, and β-actin (loading control) are shown. **j**, Immunoblots of proteins from wild-type mouse embryonic fibroblasts treated for 16 h. Biological duplicates are shown except for the siRNA-treated lanes. $n = 100$ worms per condition for lifespan analysis. *P* values for survival analysis calculated with log-rank test.

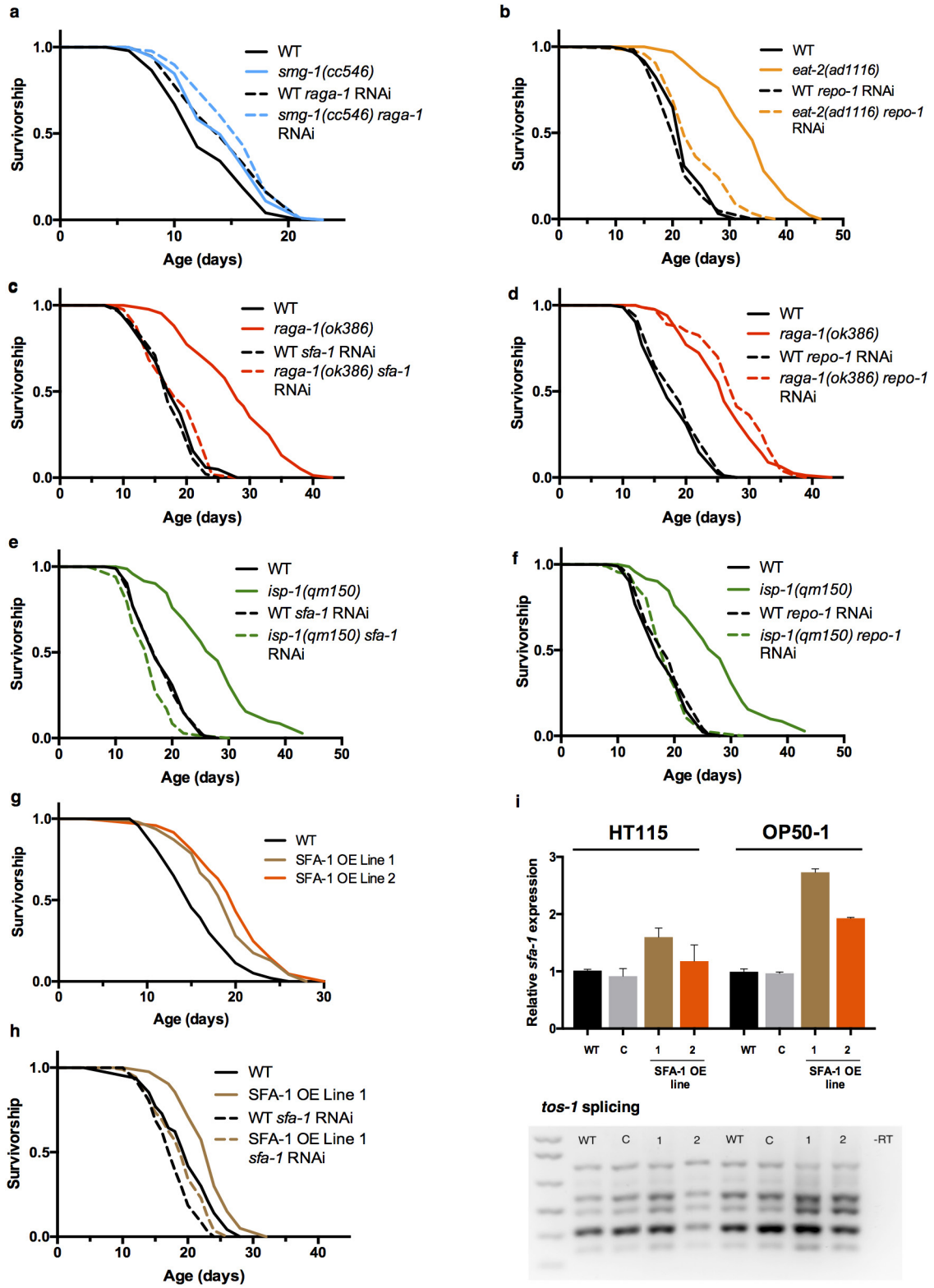

Extended Data Figure 9 | See next page for caption.

Extended Data Figure 9 | Differential effects of *sfa-1* and *repo-1* knockdown in multiple longevity pathways. a, Effect of *raga-1* RNAi in *smg-1(cc546)* mutant worms, which are defective in nonsense-mediated decay ($P = 0.041$ between *smg-1(cc546)* with and without *raga-1* RNAi, lifespan at 24 °C, Gehan–Breslow–Wilcoxon test, 3 replicates). **b**, Survival of wild-type and (*eat-2(ad1116)*) worms with *repo-1* RNAi treatment ($P < 0.0001$ between *eat-2(ad1116)* with and without *repo*-1 RNAi, 4 replicates). **c**, *sfa-1* RNAi blocks RAGA-1 mediated longevity ($P = 0.2181$, wild-type with *sfa-1* RNAi versus *raga-1(ok386)* with *sfa-1* RNAi, Gehan–Breslow–Wilcoxon test, 7 replicates). **d**, *repo-1* RNAi has no effect on *raga-1(ok386)* longevity ($P < 0.0001$, wild-type with *repo-1* RNAi versus *raga-1(ok386)* with *repo-1* RNAi, 3 replicates). **e**, Effect of *sfa-1* RNAi on mitochondrial ETC mutant *isp-1(qm150)*-mediated longevity ($P = 0.004$, wild-type with *sfa-1* RNAi versus *isp-1(qm150)* with *sfa-1* RNAi, 2 replicates). **f**, *repo-1* RNAi shortens *isp-1(qm150)*-mediated longevity to wild-type levels ($P = 0.4951$, wild-type with *repo-1* RNAi versus *isp-1(qm150)* with *repo-1* RNAi, 2 replicates). **g**, Effect of SFA-1 overexpression on wild-type lifespan on OP50-1 bacteria ($P < 0.0001$ both lines versus wild type, 3 replicates). **h**, Survival analysis of wild-type and SFA-1 overexpression lines on *sfa-1* RNAi ($P = 0.0042$, wild-type with *sfa-1* RNAi versus *sfa-1* OE line 1 with *sfa-1* RNAi, 2 replicates, $P > 0.05$, wild-type empty vector versus *sfa-1* OE line 1 with *sfa-1* RNAi, 2 replicates). **i**, Top, monitoring of *sfa-1* levels by qRT–PCR (C, injection marker control line; 1, 2, SFA-1 overexpression lines; error bars, mean + s.d. of two biological replicates for strains grown on HT115 bacteria (left); error bars, mean + s.d. of two technical replicates for strains grown on OP50-1 bacteria (right)). Bottom, *tos-1* isoform ratios with SFA-1 overexpression in day 1 adults. $n = 100$ worms per condition for lifespan analysis. *P* values of survival analysis calculated with log-rank test.

Extended Data Table 1 | Effects of splicing factor RNAi on lifespan in wild-type and dietary-restricted (*eat-2(ad1116)*) *C. elegans*

Treatment	Median lifespan N2 (days)	Median lifespan *eat-2(ad1116)* (days)	p-value N2 RNAi vs. *eat-2(ad1116)* RNAi	% Lifespan extension *eat-2(ad1116)*	FUDR
ev[*]	22	34	< 0.0001	55	+
hrpf-1	22	34	< 0.0001	55	+
repo-1	20	22	< 0.0001	10	+
snr-1	13	13	0.5147	0	+
sym-2	22	34	< 0.0001	55	+
ev	17	31	< 0.0001	82	+
sfa-1	20	20	0.9783	0	+
ev[†]	19	25	< 0.0001	32	+
hrp-2	11	11	0.1617	0	+
ev[‡]	17	25	< 0.0001	47	
uaf-2	12	12	0.0299	0	
hrp-1	18	23	< 0.0001	28	
phi-9	18	25	< 0.0001	39	
ev[§]	17	22	< 0.0001	29	
snr-2	11	13	0.3546	18	
ev[¶]	20	25	< 0.0001	25	
rsp-3	17	25	< 0.0001	47	
rsp-2	20	27	< 0.0001	35	
smu-1	17	25	< 0.0001	47	
ev	21	24	< 0.0001	14	
uaf-1	11	9	0.6094	-18	

ev, empty vector control.
*Survival curves shown in Extended Data Figs 2k, l, 9b.
†Survival curves shown in Extended Data Fig. 2m.
‡Survival curves shown in Extended Data Fig. 2n.
§Survival curves shown in Extended Data Fig. 2o.
¶Survival curves shown in Extended Data Fig. 2p.

CORRIGENDUM

doi:10.1038/nature23313

Corrigendum: Splicing factor 1 modulates dietary restriction and TORC1 pathway longevity in *C. elegans*

Caroline Heintz, Thomas K. Doktor, Anne Lanjuin, Caroline C. Escoubas, Yue Zhang, Heather J. Weir, Sneha Dutta, Carlos Giovanni Silva-García, Gitte H. Bruun, Ianessa Morantte, Gerta Hoxhaj, Brendan D. Manning, Brage S. Andresen & William B. Mair

Nature **541,** 102–106 (2017); doi:10.1038/nature20789

After publication, we noticed errors in the Source Data files for Fig. 2, Extended Data Figs 5, 6 and 9 and Supplementary Fig. 1 of this Letter. These result from data mislabelling, and have no effect on any of the figures, statistics or conclusions in the paper. The Supplementary Information to this Corrigendum contains the corrected Source Data files for the original Fig. 2, Extended Data Figs 5, 6 and 9 and Supplementary Figure 1. The original Letter has not been corrected online.

Supplementary Information is available in the online version of the Corrigendum.